Rowan University
Rowan Digital Works

Theses and Dissertations

1-25-2023

POLYETHYLENEIMINE SHELL NUCLEIC ACID NANOSTRUCTURES FROM GOLD NANOPARTICLE TEMPLATE FOR CHEMOTHERAPEUTIC DRUG DELIVERY

Brendan Guy Rucci
Rowan University

Follow this and additional works at: https://rdw.rowan.edu/etd

 Part of the Biomedical Engineering and Bioengineering Commons

Recommended Citation

Rucci, Brendan Guy, "POLYETHYLENEIMINE SHELL NUCLEIC ACID NANOSTRUCTURES FROM GOLD NANOPARTICLE TEMPLATE FOR CHEMOTHERAPEUTIC DRUG DELIVERY" (2023). *Theses and Dissertations*. 3082.
https://rdw.rowan.edu/etd/3082

This Thesis is brought to you for free and open access by Rowan Digital Works. It has been accepted for inclusion in Theses and Dissertations by an authorized administrator of Rowan Digital Works. For more information, please contact graduateresearch@rowan.edu.

POLYETHYLENEIMINE SHELL NUCLEIC ACID NANOSTRUCTURES FROM GOLD NANOPARTICLE TEMPLATES FOR CHEMOTHERAPEUTIC DRUG DELIVERY

by
Brendan Guy Rucci

A Thesis

Submitted to the
Department of Biomedical Engineering
Henry M. Rowan College of Engineering / School of Translational Biomedical Engineering and Sciences
In partial fulfillment of the requirement
For the degree of
Master of Science in Biomedical Engineering
At
Rowan University
December 12, 2022

Thesis Chair: Mark Byrne, Ph.D., Professor and Dean, School of Translational Biomedical Engineering and Sciences, Department of Biomedical Engineering, Rowan University

Committee Members:
Vince Beachley, Ph.D., Associate Professor, Department of Biomedical Engineering, Rowan University
Rachel Riley, Ph.D., Assistant Professor, Department of Biomedical Engineering, Rowan University
Jacek Wower, Ph.D., Professor, RNA Biochemistry Laboratories, Department of Animal Sciences, Auburn University

© 2022 Brendan Guy Rucci

Dedications

I'd like to dedicate this manuscript to Alexandra Jackson and Colleen Rucci, for their continued knowledge, confidence, and love.

Abstract

Brendan Guy Rucci
POLYETHYLENEIMINE SHELL NUCLEIC ACID NANOSTRUCTURES FROM GOLD NANOPARTICLE TEMPLATE FOR CHEMOTHERAPEUTIC DRUG DELIVERY
2021-2022
Mark Byrne, Ph.D.
Master of Science in Biomedical Engineering

The next generation of anticancer agents will emerge from rationally designed nanostructured materials. This work involved the synthesis and characterization of novel hollow DNA-conjugated gold nanoparticles (DNA-AuNPs) for controlled drug delivery. Polyethyleneimine (PEI) was bound to citrate-capped AuNPs, forming polymer-shell nanoparticles. Dissolution of the gold core via iodine formed hollow core polymeric nanoparticles (HCPPs) and a high density of DNA (85 molecules/particle) containing daunorubicin was conjugated. Particles were spherical with an average diameter of 105.7±17.3 nm and zeta potential of 20.4±3.54 mV. We hypothesize the DNA backbone electrostatically condensed to the primary amines on the surface of the particle toroidally, weaving itself beneath. HCPPs released 225±44.6 mg more drug/cm^3 than PEI capped AuNPs and showed release over 12 hours, an order of magnitude longer than PEI capped AuNPs. No change in release regarding DNA strand length or composition was noted. Increasing ionic concentration increased drug intercalation 64%, and intercalating drug to the DNA prior to nanoparticle conjugation resulted in 32% more drug loaded. A 10-fold decrease in the amine/phosphate ratio led to a 61% increase in drug intercalation. HCPPs did not aggregate in albumin and increased DNA stability and functionality when exposed to nuclease more than DNA conjugated gold nanoparticles. Drug delivery via HCPPs have promise to be more clinically efficacious compared to current nanoparticle designs.

Table of Contents

Table of Contents (Continued)

Table of Contents (Continued)

Table of Contents (Continued)

List of Figures

List of Figures (Continued)

Figure Page

List of Tables

Chapter 1

Introduction

The goal of this project was to synthesize novel polyethyleneimine-based hollow nanoparticles from a gold nanoparticle template that can bind DNA and daunorubicin for future chemotherapy (Figure 1.1). In addition, the research seeks characterization of the delivery platform on several physical and chemical properties to garner an understanding of how production methods influence these properties.

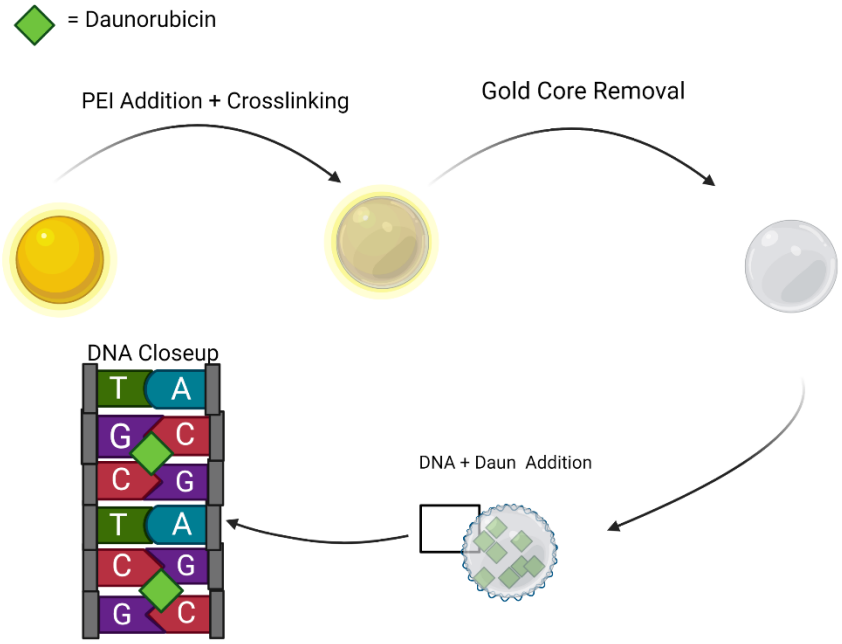

Figure 1.1. Proposed sequence of synthesis. The order of techniques used for synthesizing the HCPPs-DNA-Daun delivery platform. The steps include the addition of PEI to the gold nanoparticle surface and crosslinking once adhered to the surface. Next, the removal of the gold core through galvanic replacement. Finally, the addition of DNA and Daunorubicin to both the core of the nanoparticle and intercalated to the DNA. Figure created in BioRender.

It is hypothesized that hollow core polyethyleneimine particles with DNA and daunorubicin will maintain the morphology of the initial gold nanoparticle core, while increasing the total mass of daunorubicin loading due to the additional drug loading space in the hollow core. Additionally, differences in the stability of DNA will be observed when bound to the polymeric nanoparticle. This project builds on the known foundations of polymer, nanoparticle, and nucleic acid engineering for drug delivery purposes. By applying the principles of controlled release and molecular chemistry, we seek to develop a new vehicle for chemotherapeutic delivery.

Chapter 2 presents a brief overview of the rationale for the platform design. Chapter 3 details the methods employed to achieve these goals and synthesize the platform. Chapter 4 discusses the results of particle characterization and how these properties impact the loading and release of drug. Chapter 5 describes the profile of drug release from novel formulations and assesses the stability of DNA when bound to the hollow core polymeric particle. Finally, chapter 6 presents conclusions and proposes future experiments for this work.

Chapter 2

Background

Cancer is the second leading cause of death in the world, affecting almost 17 million individuals in the United States alone. Over the past 10 years the yearly medical costs in the United States have increased to over $157.8 billion, and with a growing number of patients being treated, the costs continue to exceed previous projections.[1] Among modern methods, chemotherapy still reigns as one of the most prevalent techniques for fully eliminating cancer from the patient.[2] Although chemotherapy is capable of directly killing tumor cells, this presents major drawbacks, as the effects are not limited to the carcinogenic tissue and can affect healthy cells. Many patients experience debilitating and life-threatening side effects due to chemotherapy, which hinders their ability to continue with treatment.[3] Therefore, there exists a need for chemotherapeutic treatment which avoids toxicity towards healthy tissue.

Next generation cancer therapies are focused on overcoming the main limitations of chemotherapy that researchers have struggled with. Dealing with the long term acquired resistance to chemotherapeutic drugs and tumor heterogeneity are the key limitations that modern strategies seek to bypass or overcome.[4] As stated previously, conventional cancer therapies are limited in their ability to directly target the desired site. Most drugs effect both the healthy and diseased tissue resulting in severe side effects to the patient. For this reason, targeted therapy has become a highly desirable quality for researchers seeking to minimize the off-target effects of therapy.[5] Antibody-targeted therapy, small molecule targeting, and ligand-targeted therapies have all been heavily utilized to directly target the

desired site. However, this does not contribute to overcoming the heterogeneity of cancer cells and the inherent drug resistance. Nor does it contribute to overcoming the high interstitial fluid pressure found in tumor cells which limits the uptake of drugs and therapeutics.[6]

Targeted therapies are reliant on the ability to connect with specific biomarkers displayed by the tumor cell, which can result in serious detrimental effects to the therapy. The tumor could mutate during treatment and reduce the presence of the biomarkers or not produce said biomarkers in the first place, making it strikingly difficult to create a therapy unique to the patient.[7] Biomarkers are also susceptible to multidrug resistance which can arise on tumor cells. The use of several drugs together may result in the creation of a new line of tumor cells forming which hold natural resistance to the biomarker and drug used in tandem to provide the therapy.[8] For this reason, new therapies seek to create platforms which can target multiple forms of cancer. Nanomedicine has garnered attention for its broad capabilities as a targeted therapeutic delivery tool.

2.1 Nanoparticles as Biomaterials

To combat the disadvantages of chemotherapy, novel methods must be implemented to improve the conditions that patients suffer through. The use of nanoparticles has been shown to increase the effectiveness and control of delivery for chemotherapeutic drug delivery.[9] Nanoparticles are submicronic colloidal systems that are made of solid organic or inorganic materials. Several morphologies and chemical compositions of nanoparticles exist, each serving a specific niche of usage.[10] Nanoparticles present a nanoscale platform in which modifications can be made to limit the effects on

surrounding healthy tissue and deliver directly to the interior of the tumor cells. This platform is unique in that it is small enough to naturally transport through cell membrane without the aid of active transport. These treatment methods have also been shown to be effective in later stage cancers.[11] Further modifications made to nanoparticles can be used to increase cell transfection, endosomal escape, or active targeting capabilities of the nanostructure.

2.1.1 Properties and Usage of Nanoparticles

Nanoparticles show different mechanical properties relative to the bulk materials they are derived from and even larger forms of particles of the same material. Nanoparticles have well understood basic mechanical properties such as hardness, elastic modulus, adhesion, and friction, which make them highly desirable tools for lubrication and nanomanufacturing.[12] Nanoparticles are also used heavily in medical imaging due to their small size and exhibition of the enhanced permeability and retention effect (EPR) in tumors. This important characteristic allows for nanoparticles to easily enter the interior of tumor cells through their microenvironment passively, allowing them to be used as points of detection within tumors for imaging.[13]

Nanoparticles possess several unique qualities which allow them to provide benefits when used for controlled drug release. They can protect the drug payload from degradation and enable sustained drug release, as well as decrease clearance and increase the accumulation of drug in the target site.[14] There are several biological barriers that nanoparticles must overcome to effectively deliver to the interior of the damaged tissue. These include renal clearance, degradation, the extracellular matrix, cell membrane,

lysosome, and membrane pumps.[15] Although, nanoparticles are unique in that they can be modified using polymers to overcome these barriers.

However, nanoparticles contain a level of toxicity that threatens their use as biomaterials. Usage in the respiratory, lymphatic, and central nervous system must be done with caution as studies have shown that exposure to nanoparticles can reduce the strength of the immune system in both animal and human subjects.[16] Therefore, proper toxicological assessment of nanoparticles must continue alongside the development of novel pharmacological systems.[17] Many different forms of nanoparticles exist with their own physiochemical properties which are unique to the material that comprise the nanoparticles.

2.1.2 Metallic Nanoparticles

One form of nanoparticles used primarily for imaging and drug delivery purposes are metallic nanoparticles. These compact agents have unique physiochemical properties as compared to their bulk materials that arise due to the high surface-to-volume ratio.[18] In order to fully utilize the full potential of these particles they must be stable and biocompatible. Nanoparticles are typically categorized in their stability using several metrics of analysis. The most crucial properties needed to understand the stability of the platform are aggregation, chemical composition, shape, size, and surface chemistry. The ability to maintain these physiochemical properties are what constitutes stability in metallic nanoparticles.[19] Magnetic metallic nanoparticles, such as iron, gold, and silver, can be effortlessly conjugated with surface coatings through electrostatic self-assembly. This makes them highly desirable as vectors for molecular diagnostics and non-invasive therapies.[20] These nanocarriers can be designed in a way to facilitate their usage for

visualization of cellular function as molecular imaging probes. These probes can help researchers understand molecular processes without disrupting or damaging the organisms being studied. [21]

Metallic nanoparticles also provide a platform to modify the therapeutic outcomes of modern chemotherapy. Nanoparticles can exploit the pathophysiology of the tumor microenvironment to improve the therapeutic outcomes for oncological therapy by targeting the overexpressed receptors on tumor cell surfaces using nanocarriers outfitted with targeting ligands.[22] A range of metallic nanoparticle-based therapies have been approved for selective tumor types and even more are preparing to enter clinical trials.[23]

2.1.3 Gold Nanoparticles

Gold nanoparticles have seen vast clinical use in cancer therapy. These particles have seen increased usage as photothermal, imaging, as well as drug delivery tools in recent years.[24] Photothermal therapy is a form of therapy in which the nanoparticles are integrated into a tumor then heated from the exterior by a laser to heat and destroy the tumor.[25] This is possible due to key mechanical properties held by gold nanoparticles: small diameter for tumor penetration, high biocompatibility, and ability to absorb infrared light. These properties also allow it to be used extensively as an imaging agent. Gold nanoparticles are capable of both passively and actively targeting tumor cells, and combined with their ability to absorb X-ray waves, allows it to provide sharp contrast in tumor imaging.[26] Another key functionality of gold nanoparticles is their high tunability, allowing for ease in the synthesis and characterization process. Their negative surface charge allows for modifications through electrostatic interaction.[27] Biomolecules like targeting ligands,

polymers, drugs, and DNA can be easily loaded to the surface of the solid particles. As a drug delivery tool, gold nanoparticles provide a platform with highly accurate control over particle size, shape, and surface chemistry. This makes gold nanoparticles an ideal resource for drug delivery. By modifying the reducing agents and pH of the reacting mixture, gold nanoparticles can be synthesized with a precise size, morphology, and polydispersity.[25] Notably, gold nanoparticle nucleic acid formulations have been developed which can provide both a targeted drug delivery and photothermal therapy to carcinogenic tissue.[28]

The facile modification of these particles combined with their innate controlled nanoscale morphology provides enough scaffolding for drug conjugation. However, gold nanoparticles present an inherent cytotoxicity. Bulk gold is chemically inert and has been seen clinical usage as an anti-inflammatory agent to treat rheumatoid arthritis.[29] On the other hand, gold nanoparticles have seen adverse outcomes *in vitro* such as organelle and DNA damage, apoptosis, and mutagenesis.[30] Though this does not give full insight to the full scope of effects *in vivo*, it gives a basic understanding of the toxicity caused by gold nanoparticles at a cellular level. Studies have shown that small (3-5 nm) and large (50-100 nm) are nontoxic to mouse models, although intermediate sizes (18-37 nm) were associated with major organ damage to the liver, spleen, and lungs specifically.[31,32] However, other studies have indicated that with minor adjustments to the surface chemistry of the gold nanoparticles, they are essentially nontoxic.[33,34] This discrepancy in findings presents a need for further investigation into the toxicity of gold nanoparticles in specific compositions on individual lines of cells. Most studies focus on simple gold nanoparticle structures with little to no modification and thus efforts to understand the nanotoxicity and pharmacokinetics of drug delivery must be evaluated on a case-by-case basis.[35]

2.1.4 Polymeric Nanoparticles

Another frequently used material for drug delivery is polymeric nanoparticles. Biodegradable polymers such as polylactic acid, polylactic-co-glycolic acid, polyethylene glycol, and polyethyleneimine (PEI) are all frequently used for their ability to encapsulate therapeutic compounds.[36] Polymeric nanoparticles have also received attention for their ability to target tissue, carry nucleic acids, and sustain release of their payloads.[37] In addition, polymeric nanoparticles are preferred over metallic nanoparticles because they are biocompatible, non-immunogenic, and avoid renal and other drug clearance systems.[38] Using the controlled release system of polymeric nanoparticles also helps to reduce the frequency of drug dosing and increase patient compliance. These platforms also increase the total potency of the drug by improving the solubility, permeability, and bioavailability of the encapsulated drug.[39] Overall, polymeric nanoparticles can serve as both a protective and mobility aid for targeted drug therapies.

For oncological therapies, polymeric nanoparticles have shown major success in chemotherapeutic delivery and gene delivery. Hydrophilic, blood compatible biodegradable polymers provide a ring of hydrophilic chains on the outer surface of the payload to prevent the phagocytosis and opsonization of the foreign body.[40] Therefore, the amphiphilic drug delivery system containing an anticancer agent will have increased systemic circulation time and an increased compatibility with the blood.[41] Since a major obstacle of chemotherapy is the need to deliver large doses to overcome rapid clearance, and the inability to deliver large doses due to toxicity, polymeric nanoparticles can serve as a mediator for release. This can be done in response to several triggers at the delivery site including targeting aptamers, pH, and temperature.[42] Polymeric nanoparticles can also

capitalize on the anatomical differences in tumors to directly target the tumor site. Since tumors are more heterogenous and contain dense leaky vasculature, polymeric nanoparticles can passively accumulate and enhance the concentration of therapeutic agents in the tumor. Furthermore, the nanoparticles can be similarly outfitted with targeting ligands, as metallic nanoparticles are, to actively target the tumor site through specific binding to the cell surface receptors and take advantage of overexpressed receptors on different lines of tumor cells.[43]

2.1.5 Polyethyleneimine Nanoparticles

PEI nanoparticles have received praise for their facile synthesis compatibility with other bioengineering materials. PEI carries a high cationic charge which serves to condense several biomolecules, including, to the surface of the particle, allowing for high loading capacity and high transfection activity (Figure 2.1).[44] Due to the high susceptibility to degradation, nucleic acids must be shielded from outside forces until they reach their destination. PEI is effective in buffering changes in pH, temperature, and charge and preventing fragile nucleic acid from being damaged when loaded to the surface of a PEI based nanoparticle. [45]

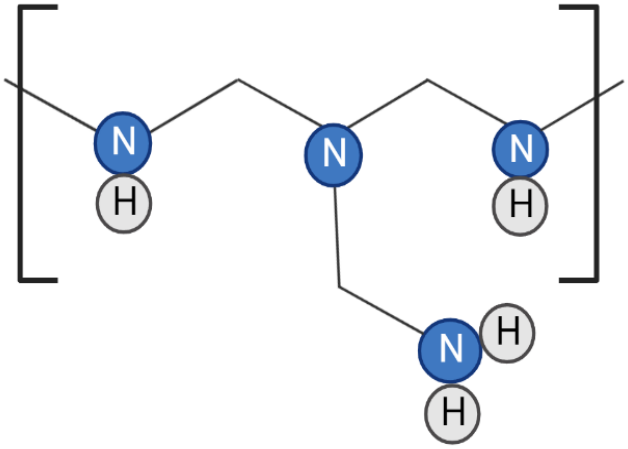

Figure 2.1. Molecular structure of branched polyethyleneimine. Polyethyleneimine, a highly cationic polymer, is typically used for its capabilities as a cell transfection agent and charge shield. Figure created in BioRender.

In terms of chemotherapy, PEI nanoparticles have been researched for many techniques including photothermal therapy, gene therapy, drug delivery, and combinatorial therapies. PEI has been shown to be capable of loading chemotherapeutic drug daunorubicin and maintain stability of the nanoparticle and therapeutic.[46–50] This anticancer agent works by stopping further growth of tumor cells though the blockage of proliferation enzyme CREB3L1.[51] Release of the daunorubicin can be induced from the PEI particles by internal changes like pH and temperature, or external stimulation by laser. PEI is typically co-delivered alongside nucleic acids as they synergistically reduce the innate tumor resistance while suppressing tumor proliferation.[50,52] PEI is a unique solution to drug delivery barriers due to its innate charge and buffering capacity. Recent contributions to the list of PEI based particles for chemotherapeutic treatment include stimulus responsive gene vectors, antibody guided targeted delivery, and co-delivered nucleic acids for gene therapy.[53–55]

2.2 Polymeric Modifications in Nanoparticles

Metal nanoparticles are often conjugated with protective shells to create core-shell hybrids which hold unique emergent properties. Gold nanoparticles have been prepared with several protective coatings in order to increase their stability and limit the aggregation of particles using several different functional groups and polymers.[56–58] Polymer coated metallic nanoparticles have also been shown to have significantly lower systemic toxicity than their bare counterparts, as well as longer circulation times when paired with known stealthing agents.[59,60] Polymers are also capable of acting as buffering agents in terms of both pH and temperature, protecting the interior metallic particles while degrading at a fixed rate relative to the polymer and influence of the surrounding environment.[61] Many polymers have been heavily studied and engineered for the purpose of protecting metallic nanoparticles and increasing their effectiveness.

Polyethyleneimine (PEI) is a polymer that has shown great capabilities in terms of promoting the cell transfection of nanoparticles and as a vehicle for drug delivery.[62–64] The cationic polymer provides a positively charged surface for negatively charged drugs to adhere, as well as improve transfection with the negatively charged cell membrane. When functionalized onto the surface of nanoparticles, this vastly improves the efficiency of drug delivery.[65] These particles are limited in their ability to bind drug to the surface. PEI nanoparticles can improve both the loading capacity and control of release of drug delivery.[66] By improving on the loading, delivery, and release rate of chemotherapeutics as compared to radiative or injectable therapies, the minimization of off target effects and efficacy of therapy can be improved. PEI has been used as a modification to gold nanoparticles to increase drug delivery efficiency. The addition of PEI to the surface is

highly controllable and the concentration of PEI can be used to synthesize diverse sizes and surface charges. Facile crosslinking of PEI conjugated nanoparticles can be further used to improve colloidal stability of the nanoparticle (Figure 2.2).[67] The gold surface can be easily tuned using PEI to improve its capabilities as a drug delivery vector.

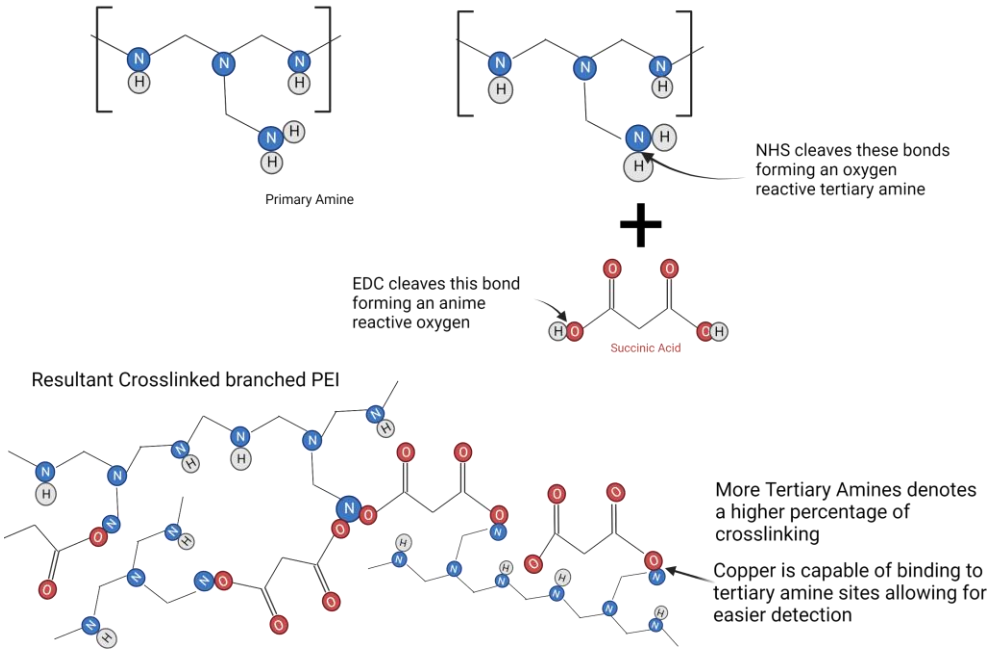

Figure 2.2. Facile "one pot" polyethyleneimine crosslinking procedure. Crosslinking procedure of branched PEI to a denser crosslinked structure, improving the overall stability when on the surface of the nanoparticle. This method of crosslinking utilizes an organic dehydration reaction with NHS to cleave the N-H bond of the PEI. EDC further cleaves the O-H bond of the succinic acid, which binds to the open amine on the PEI. This results in PEI molecules on the surface of the particle with a higher overall molecular weight. Figure created in BioRender.

PEI is able to influence the surface charge of the gold nanoparticles to increase the ability of drug loading as well as better control over endosomal escape.[68] PEI is explicitly reactive to changes in pH and temperature, allowing it to be manipulated using outside sources for the purposes of inducing drug release in the target area.[69,70] Since PEI is a polar polymer, it is an ideal target for hydrophobic drugs to help increase their solubility, allowing for denser binding to the delivery system.[71] The polymer is strongly charged and overcomes the charge of the metallic nanoparticle, causing it to dominate the interaction with the loaded drug. Nanoparticles outfitted with PEI have been shown to increase their

capacity for drug adsorption while extending the release of drug from nanoparticle systems.[72,73] Recent developments by Prajapati et al. and Mdlovu et al. have shown improvements of cell transfection of both metallic and polymeric nanoparticles capped with PEI.[74,75] This polymer is incredibly responsive to chemical and physical stimuli, allowing it to react to changes specifically in tumor microenvironments.

2.2.1 Effects of Crosslinking PEI

Crosslinking surface functionalized PEI can improve the physical characteristics of the polymer, as well as increase the stability of the polymer coating on the surface of a metallic nanoparticle. Several methods exist to densely crosslink PEI; however, EDC coupling, which utilizes disulfide intramolecular bonding, has shown frequent use amongst nucleic acid delivery carriers.[76] Crosslinked nanoparticles exhibit features like branched polymers in that their mass is spread over a larger volume and area as compared to linear forms of the same molecular weight. This results in increased rigidity and fluid retention and the reduction of pores in proportion to the density of crosslinking.[77,78]

Crosslinked PEI has been shown to be more effective in improving endosomal escape of nucleic acids as compared to free PEI of the same weight.[63,79] In terms of nucleic acid cell transfection, disulfide crosslinked PEI complexes are highly efficient in improving the membrane transfer of nucleic acids into the cytosol, while protecting the loaded nucleic acid from reducing agents.[80] PEI is typically referred to as a smart drug delivery system due to its ability to react to stimuli, and crosslinking low molecular weight PEI increases the “intelligence” of the system when binding to nucleic acids.[81,82]

Crosslinking polymers have also been shown to extend the release of small molecules from the interior of polymeric nanoparticles.[83]

2.3 History of Nucleic Acid Drug Delivery

Nucleic acids have been heavily researched and modified to become efficient drug carriers.[84] Presently, seventeen nucleic acid therapies have been approved by the Food and Drug Administration or the European Medicines Agency. This includes gene therapy, vaccine, and drug delivery purposes.[85] These structures prove to be highly efficient in drug delivery as they are highly tunable platforms. Modifications to their immunogenicity, targeting capabilities, and responses to stimulus can all improve their capabilities as drug vectors.[86]

2.3.1 Barriers to Nucleic Acid Delivery

Nucleic acids face a large concern in that they are enzymatically unstable and provoke an immune response. Additionally, unmodified nucleic acids are too hydrophilic for cell uptake and encapsulation of payloads.[87] This creates a barrier in the delivery of nucleic acids, as they cannot freely circulate within the bloodstream, nor can they naturally be uptaken by cells. To combat the intrusion of foreign DNA the body can respond with a variety of primary immunological responses.[88] One of the most common reactions to this are groups of nucleic acid receptors which restrict nucleic acid functionality and replication. Of these receptors, the enzymes known as nucleases break down both wanted and unwanted DNA.[89] Avoiding these enzymes is crucial to delivering a functional nucleic acid capable of maintaining its payload.

In response to this, several materials have been utilized to increase the potency of nucleic acids as a drug delivery vessel. Synthetic vectors of nucleic acids are hindered by their ability to accelerate the movement of nucleic acids through the cytoplasm and across the cellular membrane.[90] Polymeric nanoparticles have been used for the delivery of nucleic acids for several decades.[91–95] Polymeric nanoparticles increase the stability of nucleic acids while decreasing the immunogenicity of the delivery vessel.

2.3.2 Nucleic Acid Nanocarriers

Gold nanoparticles provide an effective scaffold for nucleic acid drug delivery due to several mechanical properties. Gold nanoparticles are fabricated with a low size dispersity and retain their functionality even when bound to several layers of nucleic acid and targeting agents.[96,97] The facile synthesis of both covalent and non-covalent AuNP conjugates with synthetic and organic DNA makes these an attractive platform for nucleic acid delivery.[98,99] However, gold nanoparticles are limited in that they are highly negatively charged and cytotoxic, resulting in several unwanted interactions with cells and their membranes.[100] Polymer modifications to gold nanoparticles are relatively simple and allow researchers to take advantage of the properties which benefit nucleic acid delivery.

PEI is another desirable vehicle for nucleic acid delivery as it neatly compacts the nucleic acid backbone to the free nitrogen in the PEI. This makes the uptake to cells and release from the endosomal compartment much more favorable due to the cationic nature of PEI.[101] Furthermore, PEI possesses a unique ability to prevent the deterioration of nucleic acids by buffering the changes in pH.[102] When inside the highly acidic tumor microenvironment, this buffering culminates in protons rapidly entering the endocytic

vessel which encapsulates the nanoparticles. The disparity in protons between the inside and outside of the vesicle drives osmosis into the interior of the endosome.[103] This "proton sponge effect" allows for nucleic acid to be delivered solely to the tumor microenvironment, as it has a naturally acidic pH. This protects the healthy tissue in the surrounding area from the harm of cytotoxic drug delivery and makes an overall more efficacious treatment.

2.3.3 Nucleic Acid Intercalators

Not only do sequences of DNA possess potential for gene delivery to manipulate cells for therapeutic purposes, but the base pairs of DNA also provide ample space for the intercalation of specific molecules. One such molecule, daunorubicin hydrochloride, also known as daunomycin, is frequently used clinically for chemotherapeutic purposes. This drug was developed and used clinically in trials as far back as the 1970's.[104] Daunorubicin can intercalate to the base pairs of DNA (Figure 2.3). The drug functions as an anticancer agent through the disruption of mitochondrial homeostasis, thus inhibiting ATP synthesis.[104] This drug has been approved for chemotherapeutic usage by the FDA since 1996 with the novel liposomal daunorubicin platform developed by Galen Partners©.[105] Additionally, the intercalated drug has been shown to improve the stability of the DNA backbone through the reduction of backbone flexibility.[106] This known change in geometry can be vital in synthesizing DNA vectors with a desired morphology.[107] The release of the drug can further be extended by modifying the architecture of DNA. By layering and twisting DNA, the amount of times the drug is exposed to intercalation sites, thus extending the release from the DNA.[108,109] Overall, this drug is highly effective in binding to DNA

and has previous clinical use as an anticancer agent, though more efficient methods of release can still be developed.[110]

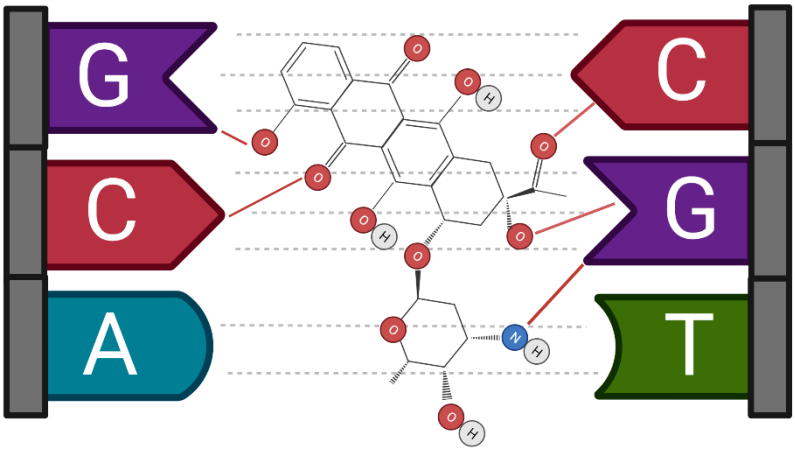

Figure 2.3. Daunorubicin intercalation to DNA nucleotides. Daunorubicin requires 3 base pairs of double stranded DNA to form a binding complex using all 5 of its binding sites (shown with red lines). The drug preferentially binds between adjacent GC base pairs and requires a buffering space of an A-T base pair as a part of the triplet sequence. Figure created in BioRender.

2.4 History of Hollow Core Particles

The coating of nanoparticles allows for dual function of both the interior particle, called the core, and the outer layer, called the shell. These core-shell nanoparticles can either retain their individual material functions, or the modification can lead to emergent properties of both the shell and core. However, these structures are limited in their storage capacity, and so, geometric modifications are needed to improve the functionality of the architecture.[111] One such structure, hollow core nanoparticles, are ideal for increasing the volume available for drug loading. These are typically crafted through layering the desired shell over a hard template, followed by removal of the core through dissolution.[112–114] This

leaves a hollow nanostructure with the mechanical and chemical properties of the initially layered shell. The development of these structures had been led by the Mirkin group with their research into polymeric-metallic hybrid nanoparticles, eventually leading to the synthesis of nanoparticles with block copolymer shell structures.[115–117] The Mirkin group has continued to expand on these novel formulations to this day with their tunable polyethylene glycol shell nanoparticles for nucleic acid delivery.[118]

2.4.1 Biomedical Applications

Hollow core nanostructures have vast potential when utilized as biomedical nanomaterials. The main applications of these particles are within the fields of bioimaging, gene delivery, and drug delivery.[111] The use of low cytotoxic polymers as shells allows for high biocompatibility and facile conjugation to the desired payload, as well as responsiveness to external stimuli.[119] Hollow metallic nanoparticles are frequently used as imaging contrast agents. They are capable of strongly absorbing near infrared light, allowing them to be easily detected, as well as heated for a photothermal form of therapy to the contrasting region.[120,121] Delivering genetic material is another key function of hollow nanostructures. Hollow structures have shown better transfection efficiency than solid nanoparticles coated in the nucleic acids.[122] This can be attributed to the multiple layers of shell that allow for more flexible loading in a less dense nanostructure. Furthermore, drug delivery applications are more effective for similar reasons, the encapsulation during synthesis and core removal process provides a larger volume for the payload and protection from outside contaminants. These structures are also capable of drug release by external forces as a shell only particle is more susceptible to the impacts of outside stimuli.[123]

Cationic polymer hollow core nanostructures are frequently used along with nucleic acids as they can condense them while maintaining their unique characteristics. Since nucleic acids are highly susceptible to immunological recognition and renal clearance, stealthing polymers are desirable to improve the effectiveness of reaching the target tissue without disrupting the integrity of the nucleic acid architecture.[124] Several hollow structures have been prepared with a range of nucleic acids to determine the relative changes in gene transfection and delivery rate based on the density of polymer used for the size of the shell.[125]

2.4.2 Colloidal Templates

Hollow core nanoparticles were first developed in 1998 by Caruso et al. when hollow silica particles were created using electrostatic self-assembly on a colloidal surface.[126] Gold nanoparticles have shown frequent usage as the template for hollow core particles due to their high stability. Gold nanoparticles can be synthesized with precise morphology and size; when these particles are coated and the core is removed, it yields a structurally intact hollow capsule, with the inner size governed by the morphology of the template.[127] Covering the gold nanoparticle in the polymer also holds the advantage of preventing one of the major drawbacks of gold nanoparticle usage, aggregation.[128] Gold is also convenient to use as a sacrificial core, as it can be easily etched using galvanic replacement with the help of inexpensive chemicals.[129]

Further developments utilized solid AuNPs as the core for electrostatic assembly of shell nanoparticles, using several etching techniques to eliminate the gold interior. [130–132] The Mirkin group has further discovered usage of AuNPs for the creation of nucleic

acid based hollow nanostructures for use as densely packed vectors for gene delivery.[133] These particles hold the major benefit of being able to replicate the morphology of the template particle when crafting the shell particle. In most cases, hollow core particles retain the shape of their template, allowing for the creation of highly uniform nanostructures.[66]

2.4.3 Polymer Shells

Mesoporous polymer hollow core particles have seen development from colloidal templates. These particles rely on the increased surface area obtained from removing the core of the particle to increase the potential as a drug vector.[134] In these spaces, several forms of shell structures have been designed including “golf ball,” “egg-yolk,” and “rattle-type” shapes.[135–137] These forms all provide a similar function in which the shell acts as a protective layer for the delivery of an interior payload.

PEI is an ideal candidate for these forms of structures, as the polymer can protect the payload from renal clearance and immunological response. PEI can act as a soft template for further layering of nucleic acids to the hollow core structure's surface. Recent studies by Liu et al. have identified hollow core PEI nanoparticles as efficient drug vectors for cancer immunotherapy, extending the release of drug in mouse models.[138]

The release profiles of drug from polymeric hollow core nanoparticles have been well studied. Release from these particles is governed by diffusion from the interior and degradation of the polymer shell.[139–141] Researchers have shown that hollow core polymeric nanoparticles can tune the release of payloads from the interior of the particle.[142] At high loading capacities, drug precipitates between the surface polymer and outer surface resulting in a high amount of release. Furthermore, thick layers of polymer shell increase

the path length required to diffuse from the interior of the particle, resulting in an extended release controlled by the thickness of the shell layer.[143,144]

In this work, we seek to create hollow core PEI nanostructure for the delivery of nucleic acid bound daunorubicin using an AuNP template. This culminates in a particle that can hold the morphology of a gold nanoparticle template while providing ample spacing of a hollow particle in the interior for drug and nucleic acid loading. The resulting particle is hypothesized to display the physical characteristics of the sacrificial gold template while providing the chemical qualities of the PEI shell.

Chapter 3

Methods

This research was conducted using several researched methods for the synthesis and characterization of nanoparticles containing polymers and nucleic acids. This section describes the methods used to load drug, determine the affinity of the drug for specific DNA sequences, and prepare the samples for an array of characterization experiments.

3.1 Materials

Spherical Gold Nanoparticles (AuNPs,15nm, 0.001-0.01%) were purchased from Ted Pella (Redding, California, USA). Copper II Sulfate ($CuSO_4$, Anhydrous), Succinic Acid (SA, ≥99%), (N-Hydroxysuccinimide (NHS, ≥98%), N-(3-Dimethylaminopropyl)-N'-ethylcarbodiimide hydrochloride (EDC, ≥98.0% by titrimetric analysis), Dimethyl sulfoxide (DMSO, ≥99.9% ACS), Phosphate Buffered Saline (PBS, 20X), Tris-acetate-EDTA Buffer (TAE, 25X), Tris-EDTA (pH 8.0), Agarose I™, Magnesium Chloride Anhydrous (MgCl), Hydrogen Peroxide (H_2O_2, 30%), and Iodine (I_2, 1N) were purchased from VWR (Radnor, PA, USA). Polyethyleneimine (PEI, ~25,000 MW, Branched) was purchased from Sigma Aldrich (St. Louis, MO, USA). Daunorubicin Hydrochloride (Daun, ≥98.0% (N)) was purchased from TCI (Tokyo, Japan). Sulfuric Acid (H_2SO_4, ≥95%) was purchased from EDM Millipore (Darmstadt, Germany). Deionized water was obtained from the Milli-Q® EQ 7000 Ultrapure Water Purification System (Sigma Aldrich, USA). Clear and black bottom 96 well plates were purchased from ThermoFisher Scientific (Waltham, MA, USA). All DNA strands and DNAse I 2U/500 µL were purchased from IDT (Coralville, IA, USA).

3.2 Synthesis and Characterization of Hollow Core Particles

3.2.1 PEI Coating

Citrate capped gold nanoparticles (AuNPs) were purchased at a known 15nm diameter and verified by dynamic light scattering. These particles were kept at 5°C to maintain their stability. Stable gold nanoparticles had a light pink color while aggregates formed and caused a color change to a dark purple. This was quantified using absorbance spectroscopy, as gold nanoparticles absorb at a wavelength of 520 nm.

The molecule PEI was dissolved in water at 10 mg/mL. This was determined to be the optimal concentration of PEI for DNA delivery as cited in previous methods.[145] Samples of PEI were heated until they reached a temperature of 80°C, taking 30 minutes to attain the desired temperature. AuNPs were added to the sample at a volumetric ratio of 2:1 PEI:AuNP. For our case, 333.34 µL of AuNPs were added to 666.66 µL of PEI, resulting in 1 mL of total solution. Samples were sonicated using a Branson 1800 Sonicator (Sigma Aldrich, USA), providing 40 kHz of sonic energy to the system for 15 minutes to reduce aggregation. The particles were then incubated overnight at 37°C, resulting in PEI capped gold nanoparticles (PEI-AuNPs). Following the overnight incubation, the particle size and zeta potential were determined using a Zetasizer nano zs90 (ThermoFisher Scientific, USA). The resulting solutions remained at 1 mL and displayed a slightly lighter pink than the original sample, which were quantified by spectroscopy.

3.2.2 PEI Crosslinking

PEI-AuNPs were crosslinked using an organic dehydration reaction to increase the particle's morphology and compositional stability. Succinic Acid, N-Hydroxysuccinimide,

and EDC were added in a molar ratio of 100:1:1.4:1.4 PEI:SA: NHS: EDC in accordance with previous methods.[63] Samples were sonicated at 40 kHz for 15 minutes to reduce aggregation. The particles were then incubated overnight at 37°C, resulting in crosslinked PEI coated gold nanoparticles (PEI-X-AuNPs). The resulting particles maintain the same light pink color which can be further confirmed using spectroscopy. The resultant mixture was centrifuged using an Axyspin R microcentrifuge (Corning, USA) at 13500 rpm and 37°C for one hour, then resuspended in 1 mL of Tris Buffer to purify the particles of excess crosslinking material.

3.2.3 Gold Core Dissolution

I_2 was added to the PEI-X-AuNPs samples in a molar ratio of 2:10 (I_2): PEI-X-AuNPs. The ideal molar ratio was determined through titration and examination of absorbance readings for AuNP presence. This reduced the gold particles to their ionic form through a galvanic replacement reaction. This reaction was left to complete over one hour with intermittent vortexing to provide better exposure to the interior particle. A wash was conducted to clean the sample of any excess gold or iodine. This resulted in hollow core PEI shell nanoparticles (HCPPs). The resultant solution was clear and showed no absorbance at 520 nm when measured.

3.2.4 DNA Loading

Six different sequences of DNA (RAN and AGC: 19, 31, and 43) were used (Figure 3.1). The RAN represents sequences which were randomly generated and have unknown affinity towards daunorubicin. The AGC sequence had repeating Adenosine, Guanine, and Cytosine base pair motifs. The associated number represents the total nucleotide length:

19, 31, and 43. Samples of DNA were preloaded with daunorubicin by incubating with 100 µL of daunorubicin to 20 µL of DNA for 1 hour. DNA loading to the HCPPs was done through facile electrostatic self-assembly. Samples of DNA were loaded into individual centrifuge tubes to create 1 mL of 0.3 µM DNA. To stabilize the samples, 1.5 µL of 1 M MgCl was added to the samples to create 5 mM in solution. Samples were sonicated at 40 kHz for 15 minutes to reduce aggregation. The particles were then incubated overnight at 37°C, resulting in hollow core PEI particles conjugated with DNA (HCPPs-DNA).

Figure 3.1. DNA sequences utilized. The sequences of DNA utilized in this research are denoted by their nucleotide composition and total sequence length. RAN refers to the sequences with a randomly chosen nucleotide sequence following the first 6 strands whereas AGC refers to the nucleotide sequence with a repeating AGC motif. "S" represents the thiol linker on the 5' end of DNA. Figure created in BioRender.

3.2.5 Therapeutic Loading to Nanoparticles

To load daunorubicin to the HCPPs, 100 µL of 200 µM daunorubicin was added to 1000 µL of HCPPs-DNA solution. The solution was placed in darkness on a rotator

overnight to maximize exposure of the drug to the particle surface and interior.[134] The resultant solution was bright orange in color indicating the presence of high concentration daunorubicin in solution. Initial concentration of daunorubicin in solution was determined by fluorescence measurement at excitation λ=480 nm and emission λ=590 nm. Fluorescence testing was done in a black bottomed 96 well plate (Corning, USA) in dim lighting to ensure no damage to the light sensitive daunorubicin. This resulted in hollow core PEI shell nanoparticles with DNA and daunorubicin (HCPPs-DNA-Daun). The resulting solution was a lighter orange color than when daunorubicin was initially introduced, indicating the movement of the drug to the surface and interior of the nanoparticle. Additional samples were created to use as controls for future comparison: gold nanoparticles with a crosslinked PEI coating and condensed DNA with daunorubicin (PEI-X-AuNP-DNA-Daun) and hollow core PEI shell particles with daunorubicin (HCPPs-Daun).

3.2.6 Preparation for Fourier Transform Infrared Spectroscopy (FTIR)

FTIR analysis was performed on a Nicolet™ iS50 FTIR Spectrometer (ThermoFisher Scientific, USA). To prepare PEI-AuNPs, PEI-X-AuNPS, and HCPPs-Daun for proper FTIR usage, 75 mg of $CuSO_4$ was added per 1 mL of PEI in solution. This resulted in a PEI-Cu complex on the surface of the particles which allowed for detection of the tertiary amine groups in PEI at 1630 cm^{-1}.[146] The resultant complex was a deep blue color that was visible to the naked eye and allowed for facile detection of successful PEI surface binding. This method is not viable for DNA loaded particles as the free amine groups are not available for PEI-Cu complex formation whilst DNA is condensed to the surface. Furthermore, a range of PEI-DNA complexes were studied under FTIR to

ascertain the charge ratio of primary amines to phosphate backbones. Volumetric ratios of 1-5 PEI: DNA were investigated to determine the total ratio of positive to negative charges in solution.

3.3 DNA Affinity Towards a Range of Surfaces

To examine the baseline of binding to 2D gold surfaces, gold wafers of a known size (10 mm x 10 mm) were used. Wafers were initially cleaned of any contaminants using a piranha solution containing a 3:1 mixture of Sulfuric Acid and Hydrogen Peroxide. Wafers were rinsed in ethanol then suspended in 400 µL of 0.3 µM DNA for 1 hour inside a 24-well plate. Wafers were then washed with water then coated in DTT for 1 hour to remove the bound DNA from the surface. The resulting solution was measured for absorbance at λ=260nm to detect DNA remaining in solution. The concentration was converted to molecules of DNA per cm^2 of gold surface. To examine binding to AuNPS, PEI-X-AuNPs, and HCPPs-Daun the particles were mixed and rotated overnight with 2 µM of DNA resulting in AuNPS-DNA, PEI-X-AuNPS-DNA, and HCPPs-Daun-DNA, respectively. The resulting solutions were centrifuged using an Axygen® Axyspin Refrigerated Microcentrifuge (Corning, USA) at 37°C, 10000 rpm for 60 minutes, then resuspended with 300 µL DTT for 1 hour to remove the bound DNA. The resultant supernatant was measured for absorbance at λ=260nm to detect DNA remaining in solution, and mass balance was used to calculate the total concentration bound to the surface of each set of particles.

3.3.1 Effects of Ionic Strength on DNA Binding

To understand the contribution of ionic strength on the binding capabilities of DNA to PEI, the binding at different ionic concentrations was investigated. The RAN-19 strand was used together with varying quantities of sodium chloride (NaCl) to adjust the salt content. Concentrations ranged from 200-800 mM of NaCl with increments of 200 mM. Ethidium bromide (EtBr), a fluorescent molecule that's fluorescent intensity is increased when bound to the base pairs of DNA, was used as a detection agent. When in the presence of PEI, the intensified fluorescence of the EtBr-DNA complex is quenched.[147] EtBr was added in a 1:10 molar ratio to 2 µM of DNA RAN-19. This in turn was added to a stock solution of Tris buffer and 20 µL 10 mg/mL PEI to create 1 mL of total solution. NaCl was then added in the previously mentioned concentrations to create varying ionic strengths in solution. The resulting solution was left at room temperature for an hour to allow time for binding.

The solution was then measured for fluorescence at excitation wavelength λ=520 nm and emission wavelength λ=600 nm. The relative fluorescence (F_r) was determined through comparison to the relative fluorescence of the bare fluorescent materials (Equation 1). In this equation, the fluorescence of EtBr in the absence of DNA (F_e) was subtracted from the measured fluorescence (F_{obs}), then divided by the initial fluorescence of the EtBr-DNA complex in the absences of cationic polymer (F_o), subtracted by F_e.

$$F_r = \frac{F_{obs} - F_e}{F_o - F_e} \quad (1)$$

3.3.2 Effects of Charge Ratio on DNA Binding

To understand the effect that the charge ratio has on the binding of DNA to the cationic polymer surface, a range of charge ratios were compared. The RAN-19 strand was utilized with varying ratios of 10 mg/mL PEI, thus changing the ratio of primary amines to backbone phosphates in solution. Charge ratios of 0.2-2.0 were investigated and EtBr was again used as the fluorescent agent of interest. EtBr was added in a 1:10 molar ratio to 2 μM of DNA RAN-19. This was added to a stock solution of Tris buffer and varying amounts of 10 mg/mL PEI to create 1 mL of total solution. The resulting solution was left at room temperature for an hour to allow time for binding. The relative fluorescence was calculated through the previously described equation.

3.4 Agarose Gel Electrophoresis

Gel electrophoresis was conducted in a 10 cm, Axygen® Horizontal Gel Box, (Corning, USA) using the Owl EC1000XL Programmable Power Supply (ThermoFisher Scientific, USA). A 1.2% Agarose Gel was created using a 1X TAE buffer created from 25X stock buffer. The gel was run at 100V for 1 hour using the FTIR prepared samples to create a full profile of gel permeation.[148] The difference in permeation of different DNA sequences was compared between DNA loaded with daunorubicin prior to addition to the nanoparticles and DNA loaded with daunorubicin simultaneously to particle addition.

3.5 Daunorubicin Affinity Towards a Range of DNA Sequences

A standard curve of daunorubicin concentration was created using the SpectraMax® M3 Multi-Mode Microplate Reader (VWR, USA) for later usage in determining daunorubicin concentration. DNA sequences were used to determine

daunorubicin's affinity towards them. daunorubicin and DNA were mixed at molar ratios of 10, 25, 50, 100, 250, 500, 750, 1000 per 1 mole of DNA. Solutions were left for 1 hour to allow daunorubicin to intercalate to DNA. Daunorubicin's fluorescence was measured, then through mass balance was converted to a measure of molecules of daunorubicin per strand of DNA plotted against the molar ratio of Daun: DNA.

3.6 In Vitro Drug Release

Elution of drug was conducted in 75 mL of 1X PBS prepared from a stock solution of 20X PBS in a sealed dissolution apparatus held at 37°C, with rotators providing mixing at 150 rpm. A Float-a-lyzer dialysis bag was prepared in accordance with included instructions for usage, and 1 mL of HCPPs-DNA-Daun were loaded to the interior of the dialysis bag. Five aliquots of 1 mL were taken from the PBS at time points 0, 1, 5, 10, 15, 30, 60, and 240 minutes. The aliquots were measured for fluorescence at excitation λ= 480 nm and emission λ=590 nm to determine the concentration of daunorubicin in the PBS solution.

3.7 Drug Release Model

Drug release was modeled to fit the Korsmeyer-Peppas drug release model that is frequently used to describe the diffusion of drug from polymeric nanoparticles.[149,150] The model describes a zero-order release for the first 60% of the total fractional release, followed by a first-order release for the remainder of the release profile. The model approximated the fractional release (F) of the drug at time point "t" being equal to the amount of drug released at "t" (M_t) divided by the total amount of drug (M). This was equivalent to a kinetic constant (K) multiplied by the time point (t) with a diffusion or

release exponent (n) (Equation 2). The exponent "n" defines the mechanism of drug release where a value below 0.45 is representative of Fickian diffusion, a value between 0.45 and 0.89 is indicative of non-Fickian diffusion, and n=0.89 is indicative of zero order release. All values above 0.89 represented super case II transport, where sorption is controlled by stress induced relaxations at the boundary.[151]

$$F = \left(\frac{M_t}{M}\right) = K * t^n \quad (2)$$

Release of non-polymeric nanoparticles and free drug were modeled via other methods as there were no barriers to the release of drug from the dialysis membrane to the exterior supernatant.

3.8 Assessment of DNA Stability

3.8.1 Nuclease Degradation

To compare degradation of DNA in free solution and bound to particles, the RAN-19 strands were exposed to nuclease. Samples of DNA bound to HCPPs, DNA bound to Citrate Capped AuNPs (AuNP-DNA), and freely dispersed in water were analyzed. HCPPs were crafted in accordance with previously mentioned methods in section 3.2. AuNP-DNA was synthesized through the addition of 10.7 µL of RAN-19 DNA to create 0.3 µM of DNA in a total of 300 µL solution. To stabilize the samples, 1.5 µL of 1 M MgCl was added to the samples to create 5 mM in solution. Samples were sonicated at 40 kHz for 15 minutes to reduce aggregation. The particles were then incubated overnight at 37°C, resulting in AuNP-DNA particles.

To observe the functionality of DNA as a nanocarrier, EtBr was added in the same formulation as mentioned in section 3.3.1. The baseline fluorescence of the samples was calculated following 1 hour of incubation. To simulate the degradation of DNA when exposed to nuclease, DNAse I was incorporated.[152] A total of 11 µL (corresponding to 0.0717 units) of DNAse I was introduced to the samples and heated to 37ºC and allowed to degrade the DNA for 10 minutes before incorporating 10 µL of Tris-EDTA to halt the reaction. A dilution of 0.01 M Ammonium Hydroxide was added to the nanoparticle solutions to shift the pH to 9 and slowly strip DNA from the surface of the particles over the course of 48 hours.

3.8.2 Albumin Study

To determine the stability of particles when circulating through the bloodstream, albumin was used.[153] HCPPs were crafted in accordance with previously mentioned methods in section 3.2. HCPPs were suspended in both Tris-EDTA buffer (pH 8.0) as well as bovine serum albumin at 10 mg/ml. Particle solutions were left to mix for 1 hour before being tested for aggregation through dynamic light scattering at 37°C.

Chapter 4

Particle Characterization

In this research, a facile and repeatable method was developed for synthesizing particles of the desired properties. These properties are deemed desirable for efficient and targeted drug delivery of nucleic acids for chemotherapeutic payloads. This section details the findings in terms of several metrics typically used to characterize nanoparticle stability and functionality as vessels for drug delivery.

4.1 Particle Characterization Trends

4.1.1 Particle Size and Morphology Characteristics

The particle diameter was defined through examination by dynamic light scattering (Figure 4.1). The gold nanoparticles were found to have a diameter of 18 ± 0.2829 nm. When coated with PEI, the diameter of the particles increases by 52 ± 7.3 nm. Since there is no limiting factor to the layering of polymer, there is a wider polydispersity seen within the sample.[154] When crosslinked and resuspended, the overall size and polydispersity decreases by 13 ± 4.9 nm, as excess PEI has been washed from the system. When the core is removed and drug is introduced to the system, the size increases by 8.5 ± 1.0 nm as drug is encapsulated by the hollow particle. With the loading of DNA to the surface of the HCPPs-Daun, the overall diameter increases 40.3 ± 17.3 nm with the condensation of the DNA to the surface through electrostatic interactions between the PEI's primary amines and DNA's backbone phosphates. Polydispersity is widespread as varying amounts of DNA can bind to each particle, resulting in a larger variety of particle diameters. The

changes in diameter between all sets of particles were determined to be statistically significant through one-way Anova testing.

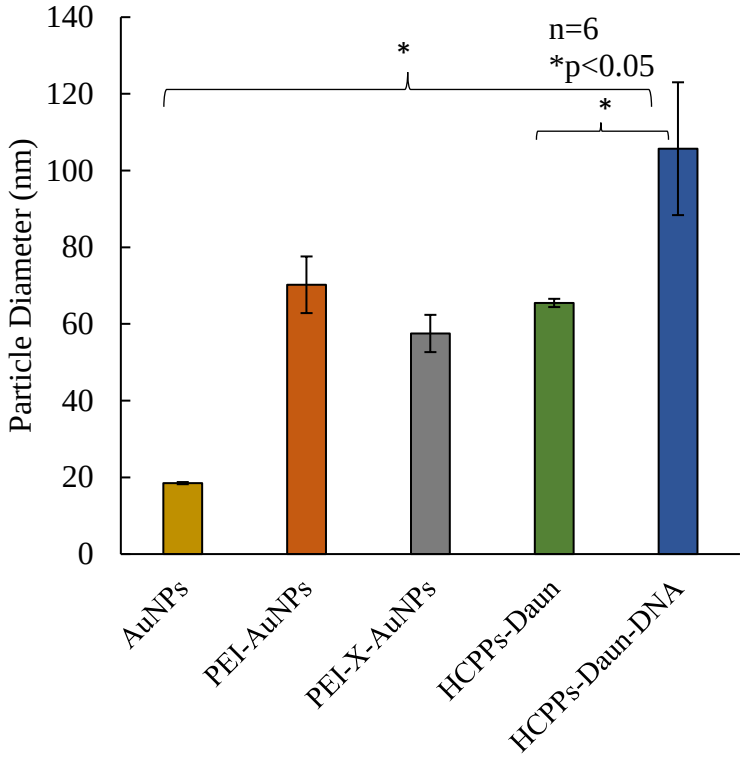

Figure 4.1. Particle diameter following polymeric modifications, core removal, drug addition, and DNA conjugation. Several configurations of nanoparticles are compared by total particle diameter: (from left to right) Citrate Capped Gold Nanoparticles (■), PEI Capped Gold Nanoparticles (■), Crosslinked PEI Capped Gold Nanoparticles (■), Hollow Core PEI Particles loaded with daunorubicin (■), and Hollow Core PEI Particles conjugated with daunorubicin loaded DNA (■). Results obtained through dynamic light scattering with consistent temperature. Results were aggregated between all DNA sequence types and data quality criteria were determined to be met through internal software of the Zetasizer. Significance was found by One-way Anova Test.

A circular and ovoid morphology can be hypothesized to have formed in samples due to the formation of a singular peak in the distribution of particle diameters (Figure 4.2). Dynamic light scattering presupposes a spherical morphology of the particles; thus, a

singular peak indicates a particle diameter of a uniform length. Citrate capped gold nanoparticles showed a small 21 nm range between the largest and smallest particle detected in solution. With polymeric addition to the surface, this range increases to 350 nm, suggesting aggregation between uncapped particles. There was no notable change in this range with the crosslinking of the surface PEI. This range increases again to 391 nm with the addition of daunorubicin to the core of the hollow core PEI particles. This increase is hypothesized to occur due to varying amounts of daunorubicin binding to the interior of the nanoparticle. There is no modification made to control the degree of drug loading to the interior of the core, thus we assume that the electrostatic binding occurs to varying extents in each particle. Finally, the DNA condensation on the particle surface increases this range to 660 nm. This is again hypothesized to occur due to differences in the loading density per nanoparticle, as there are no factors used to remove particles of high or low nucleic acid density from the solution.

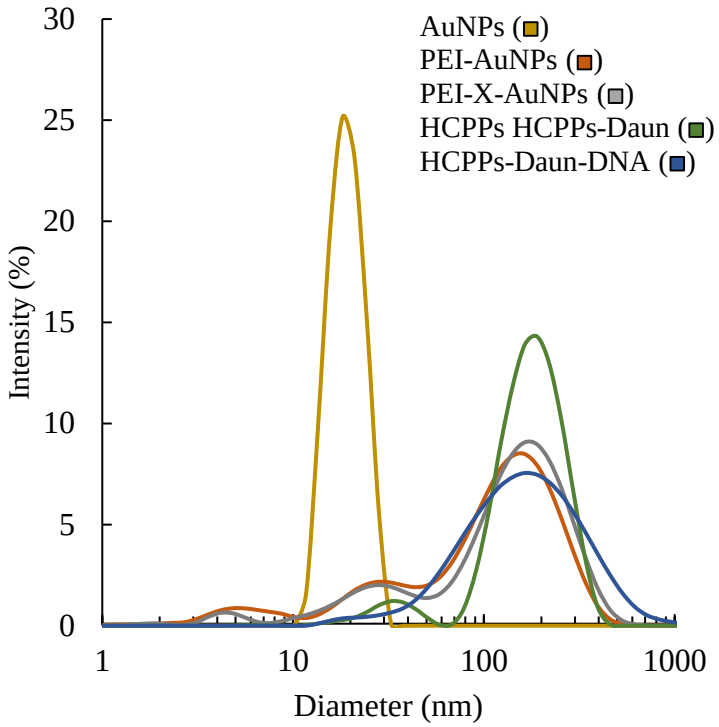

Figure 4.2. Effects of polymeric modifications, core removal, drug addition, and DNA conjugation on dispersity of particle diameters. Several configurations of nanoparticles are compared by distribution of particle: (from left to right) Citrate Capped Gold Nanoparticles (■), PEI Capped Gold Nanoparticles (■), Crosslinked PEI Capped Gold Nanoparticles (■), Hollow Core PEI Particles loaded with daunorubicin (■), and Hollow Core PEI Particles conjugated with daunorubicin loaded DNA (■). Results obtained through dynamic light scattering with consistent temperature. Results were aggregated and data quality criteria was determined to be met through internal software of the Zetasizer.

4.1.2 Particle Zeta Potential Changes

The zeta potential of each stage of particle synthesis was found through Zetasizer measurement (Figure 4.3). A highly negative ($\zeta \leq -25$mV) zeta potential was observed from the citrate capped gold nanoparticles. This was a deliberate choice by the manufacturers to prevent particle aggregation. A highly positive ($\zeta \geq +25$mV) zeta potential was obtained with the addition of PEI. This is due to the highly cationic nature of the polymer and the high charge ratio of nitrogen as compared to free phosphates in DNA.

This high positive charge can further prevent aggregation between particles.[155] With the crosslinking of PEI on the surface of the particles, there was a 7.3 ± 1.2 mV decrease in the zeta potential, as cationic primary amines were used to crosslink between PEI molecules. Incubation of hollow core particles with daunorubicin shows a further 7.7 ± 0.87 mV decrease in particle zeta potential as the daunorubicin binds to the surface and interior of the hollow core particle through electrostatic interaction, limiting the cationic primary amines on the surface of the particle. These changes were all determined to be statistically significant. The addition of DNA to the surface of the particle causes a statistically insignificant increase of 4.4 ± 3.5 mV, as DNA takes the place of daunorubicin on the surface of the nanoparticles and intercalates additional daunorubicin to the nucleotides.

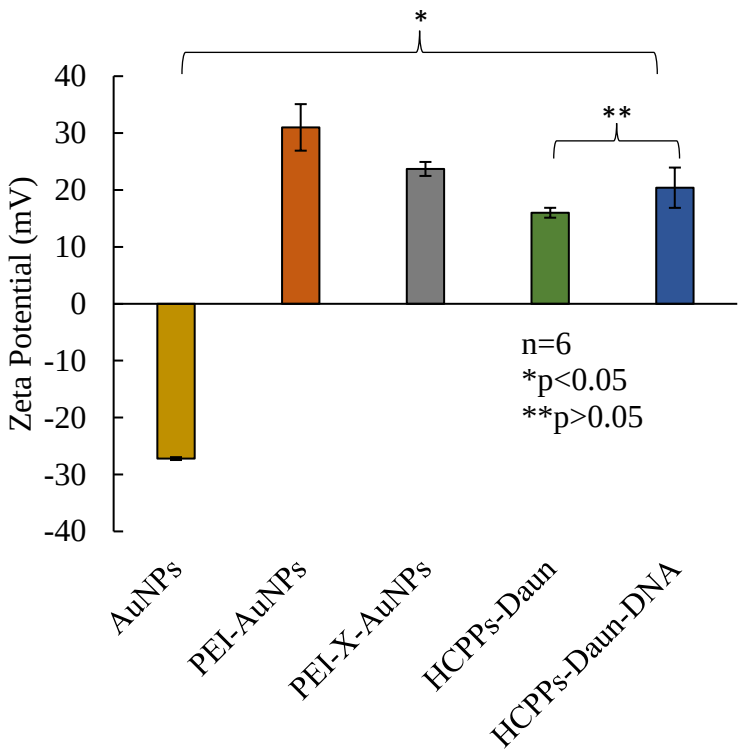

Figure 4.3. Particle zeta potential following polymeric modifications, core removal, drug addition, and DNA conjugation. Several configurations of nanoparticles are compared by zeta potential: (from left to right) Citrate Capped Gold Nanoparticles (■), PEI Capped Gold Nanoparticles (■), Crosslinked PEI Capped Gold Nanoparticles (■), Hollow Core PEI Particles loaded with daunorubicin (■), and Hollow Core PEI Particles conjugated with daunorubicin loaded DNA (■). Results obtained through Zetasizer nano zs 90 with consistent temperature with consistent temperature. Results of all DNA sequences were aggregated, and data quality criteria was determined to be met through internal software of the Zetasizer. Significance was determined by One-way Anova Test.

4.1.3 Absorbance Characteristics of Particles Following Modifications

Gold Nanoparticles are capable of being detected through absorbance measurements, allowing for facile detection of core composition and gold core removal.[156] The absorbance at between 400 and 600 nm wavelengths was noted along each step of particle synthesis (Figure 4.4). Citrate Capped Gold Nanoparticles were observed to have the highest absorbance at 520 nm. When coated with PEI the detection of gold through absorbance is diminished 56% as layers of polymer shield the gold surfaces interactions with light. This

is further diminished 75% when PEI is crosslinked on the surface, as the PEI is packed more densely over the surface of the gold. The dissolution of the gold core results in an 85% decrease of absorbance in the 520 nm point, as the gold no longer retains any optical properties it had in the colloidal phase once dissolved by the iodine. The addition daunorubicin and DNA increase the absorbance of the particles at 520 nm, however, this can be attributed to the minor absorbance displayed by daunorubicin at 480 nm.[157] The absorbance of daunorubicin in solution is not statistically significantly changed by the addition of drug loaded DNA to the surface of the particle.

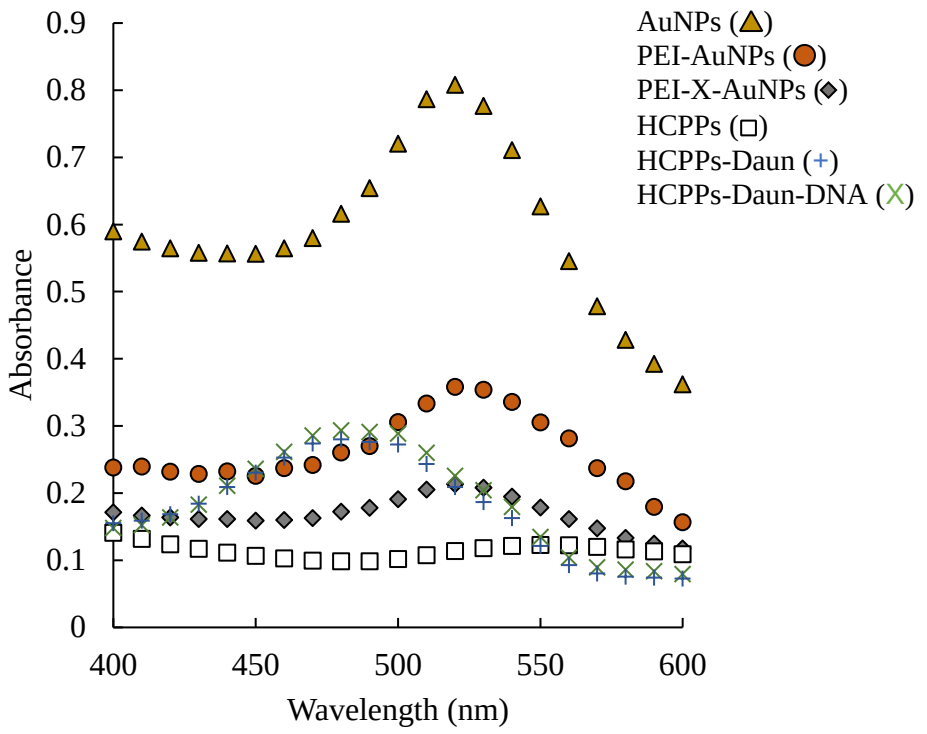

Figure 4.4. Changes in absorbance of nanoparticles following polymeric modifications, core removal, drug addition, and DNA conjugation. Several configurations of nanoparticles are compared by total particle diameter: Citrate Capped Gold Nanoparticles (▲), PEI Capped Gold Nanoparticles (●), Crosslinked PEI Capped Gold Nanoparticles (◆), Hollow Core PEI Particles (□), Hollow Core PEI Particles loaded with daunorubicin (X), and Hollow Core PEI Particles conjugated with daunorubicin loaded DNA (+). Samples measured on standard 96-well clear bottomed plates. Absorbance spectrum taken from 400-600 nm with baseline reduced by water blank. Data is representative of n=3.

4.1.4 FTIR Analysis of Polymeric Nanoparticles

Fourier transform infrared spectroscopy was used to further identify the chemical composition of nanoparticles. FTIR can elucidate the nature of bonds within a given solution. With the formation of the PEI-Cu complex, the detection of primary amines in solution is possible (Figure 4.5).[158] Primary amines which are capable of binding are detected in a medium width with a transmittance at 3500-3300 cm^{-1}. Tertiary amines which compose the backbone of the polymer are detected at 1680-1630 cm^{-1}. The transmittance

detected by FTIR shows primary amines appearing in the sample four times as often as tertiary amines. Further analysis of additional particle configurations allows further validation of the composition of the nanoparticles. These additional conformations allow for the detection of DNA and daunorubicin in solution following washes and confirms that the binding of the DNA backbone to the surface is conducted through primary amines (Figures A1-A2).

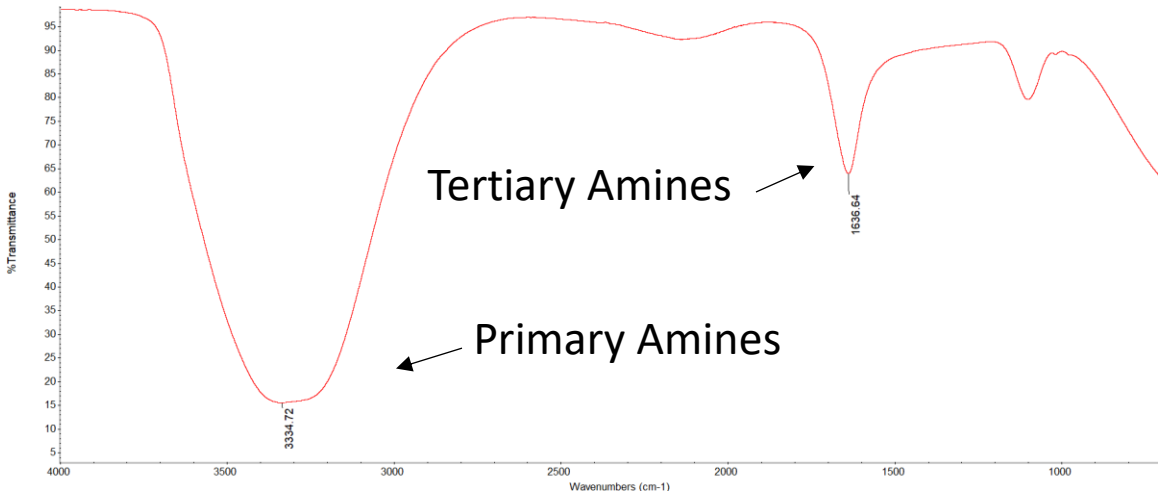

Figure 4.5. FTIR detection of the PEI-Cu complex in hollow core polyethyleneimine particles. 75 mg of copper is used per 1 mL of HCPPs. The aggregates of 32 individual runs are aggregated, and a background measurement is collected before data collection. Data points indicate the wavelength at which the peak occurs. Composition of sample determined through cross-examination of a library of Infrared Spectroscopy Frequency Ranges.

4.2 DNA Affinity Towards Gold Wafers and Nanoparticles

To better understand the capabilities of DNA binding to the hollow core polymer model, we investigated the ability of DNA to bind to several gold and polymer coated surfaces. This gave a baseline for determining how the effectiveness of DNA binding was

modified by adding polymer and removing the gold core. DNA architectures when bound to cationic polymers are highly dependent on the charge ratio of primary amines in the polymer to the number of phosphates available in the DNA backbone.

4.2.1 DNA Binding to Gold Wafers and Nanoparticles

The first form of binding substrate used was gold wafers which allowed for binding to a known surface area of gold. Wafers and nanoparticles were compared by the individual DNA strands to determine the changes in affinity regarding the composition and length of the strand (Figure 4.6). There were no significant differences in the amount of DNA bound to the gold wafer surfaces, in terms of the diverse types of stands. Length and composition of the nucleotides did not play a role in the ability or affinity towards binding to a gold surface. Between 1.5-2 x1010 DNA molecules could attach per cm2 of the gold wafer. Binding was determined through absorbance, with total number of molecules being calculated from a standard curve. Gold nanoparticles bound 2 orders of magnitude lower than the gold wafers, between 4.0-5.5 $x10^8$ molecules of DNA bound per cm^2 of gold surface area. There was no significant difference in the amount of DNA bound to gold nanoparticles based on the composition or length of the strand. The differences between the wafers and particles are hypothesized to be due to the differences in architecture of DNA binding. Previously, our group has demonstrated the production of gold nanoparticles affixed with nucleic acids in a radial confirmation.[159] However, the planar surface of the wafer results in a linear conformation of the DNA. The radial confirmation on the nanoparticle surface can limit the ability of nucleic acids to bind to the surface due to steric hindrances. Furthermore, interactions between particle bound DNA cannot be ignored and may hinder further binding to neighboring particles. Though increasing the concentration

of DNA in solution would allow us to match the density of DNA on the gold wafer, we retained the original concentration to maintain consistency across our release studies.

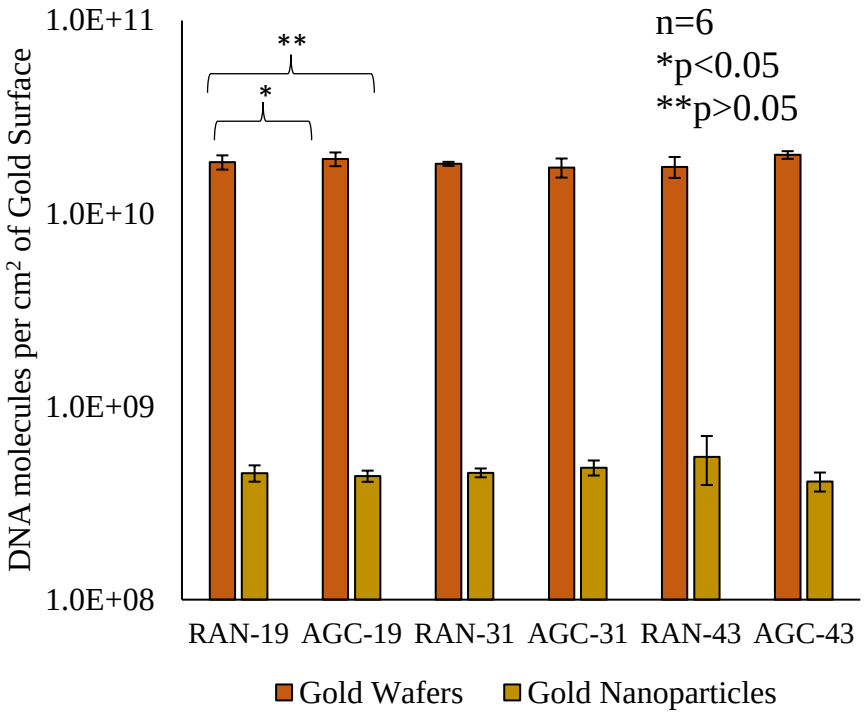

Figure 4.6. DNA bound per cm^2 of gold surface. RAN sequences and AGC sequences were compared for binding density to Gold Wafers (■) and Gold Nanoparticles (■). Significance was determined through One-way Anova Test.

4.2.2 DNA Binding to Gold and Polymeric Nanoparticles

A range of nanoparticles were used in determining the loading density of DNA strands to the surfaces of both gold and polymer (Figure 4.7). Each DNA strand was tested separately on the different particle surfaces. Gold nanoparticles were determined to have the highest density of DNA binding to the surface, reaching between 115-155 DNA molecules per particle in solution. This was found to be significantly higher than the

polymeric shell nanoparticles which ranged between 75-95 DNA molecules per particle. This can be attributed to the difference in DNA architecture of the surface of gold and cationic polymers. Gold nanoparticles with their negative surface charge allow the DNA, which is outfitted with thiol to increase binding capability, to orient in a radial structure. This uses only a small portion of the surface area to attach the DNA to the surface. DNA binding is thus limited by the repulsion of the negative DNA backbones from one another, resulting in an even spacing of DNA molecules across the surface of the nanoparticle. However, PEI surface coatings force the phosphate backbone of the DNA to electrostatically bind to the highly cationic surface of the nanoparticle, resulting in a condensed structure to the surface. Thus, a higher surface area is taken up by each DNA strand, resulting in an overall lower number of strands per particle. There was no significant difference found between the amount of loading found on the PEI capped gold nanoparticles as compared to HCPPs, as the surfaces both maintained a similar level of cationic charge. Additionally, there was no statistical significance between the binding capabilities of the DNA strands to the surfaces in terms of strand composition or length.

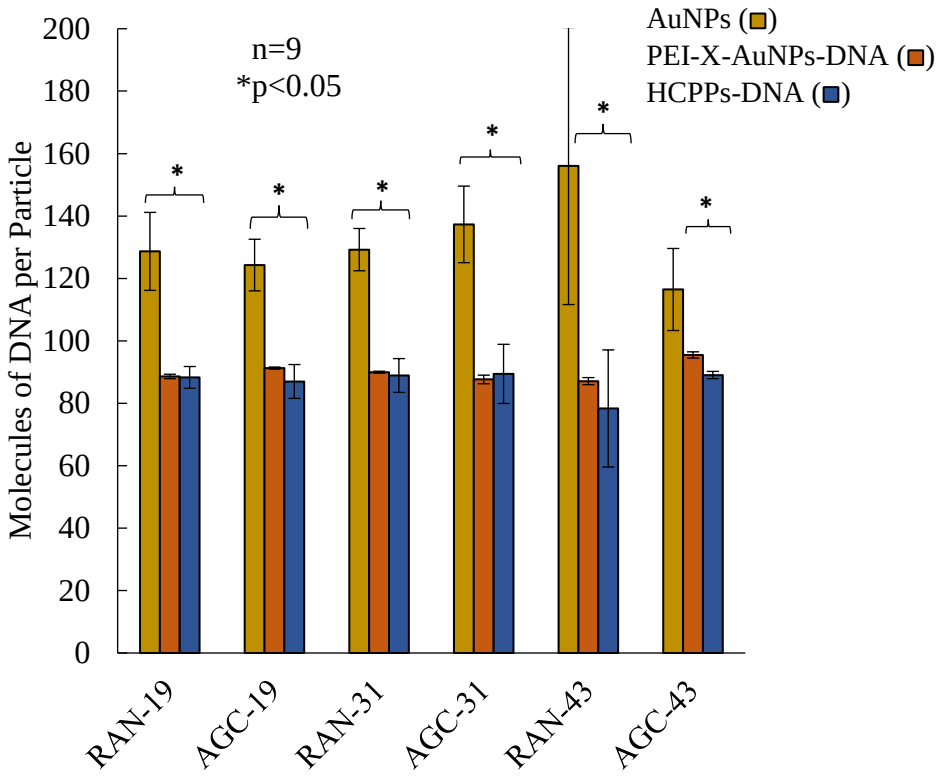

Figure 4.7. DNA binding to nanoparticles. Several configurations of nanoparticles are compared by total DNA loaded to surface: (from left to right) Citrate Capped Gold Nanoparticles ( ), PEI Capped Gold Nanoparticles ( ), and Hollow Core PEI Particles conjugated with daunorubicin loaded DNA ( ). Significance was determined through One-way Anova Test. Data is representative of n=3.

Due to the nature of the zeta potential, particle composition, and surface binding data, we hypothesize the DNA architecture on the particle to fit a toroidal model (Figure 4.8).[160] This hypothesis comes from the knowledge of several results from the data. First, the particle's surface remains highly positive throughout the changes to surface chemistry and crosslinking density. The negatively charged DNA backbone is likely to orient itself to allow for the most binding to the polymer surface. Secondly, the hollow particle comprises many primary amines, available for electrostatic binding. These amines are located throughout the particle, not just on the surface. It is then likely that the DNA would

be able to maneuver into the shell of the particle to reach more of the available amines once the surface is fully coated by a DNA layer. Finally, gold nanoparticles attach a higher number of DNA molecules to the surface. The binding mechanism for this interaction is at the DNA's 5' end, where the thiol linking cap is located. However, the polymeric nanoparticles bind DNA at the backbone, resulting in binding across any point of the DNA strand. This increases the amount of surface area that one DNA strand can coat, reducing the density of DNA molecules bound per particle. For this reason, we hypothesize that DNA condenses to the surface rather than a radial confirmation.

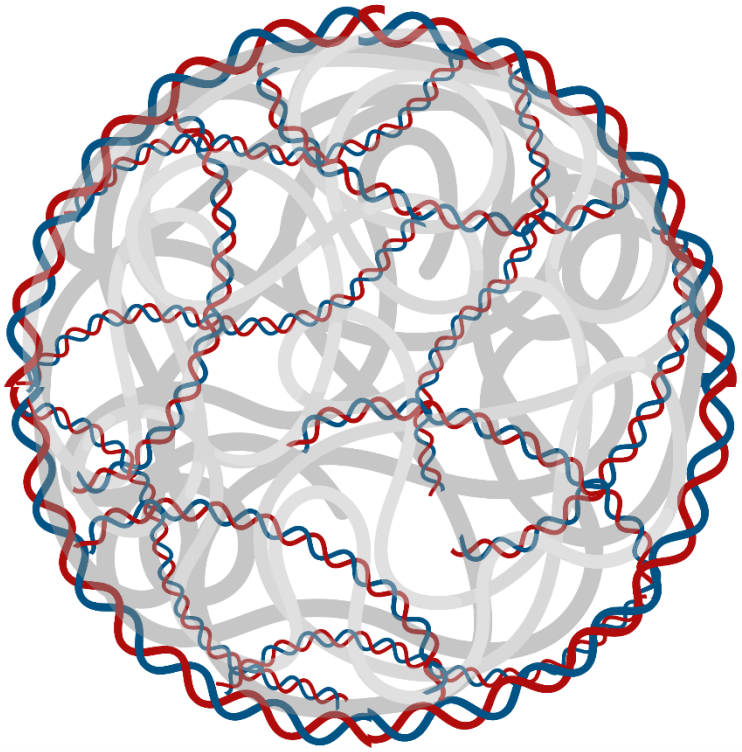

Figure 4.8. Toroidal morphology of DNA on hollow PEI particle. Proposed toroidal morphology due to the cationic charge of the polymer surface. DNA interweaves itself superficially underneath the surface to orient its phosphate backbone in line with the surface's primary amines. Figure created in BioRender.

4.2.3 Effects of Ionic Concentration and Charge Density on Drug Binding

To understand the effect of ion concentration on the capability of DNA binding to the PEI surface, several salt concentrations were utilized during the binding process under stable conditions. (Figure 4.9). Utilizing EtBr, which fluoresces in the presence of DNA and is quenched in the presence of PEI, the capability of drug binding in the presence of PEI was monitored. At lower concentrations, the condensation of the DNA to the PEI surface prevents EtBr binding to the minor groove of the DNA backbone. With increasing salt concentration, the phosphate backbone of DNA is stabilized and limits the electrostatic binding of DNA to PEI, which allows for an increase in the intercalation and formation of the DNA-EtBr complex. When increasing the ionic concentration of the solution from 200 nM to 800 nM, there was a proportional 64% increase in the relative fluorescence of EtBr. This denotes a linear relationship between the ionic concentration in solution and the potential for drug loading by nucleic acids. Furthermore, we tried to analyze the effect of ionic concentration on the nanoparticle's overall size but increasing it above 200 nM resulted in a high degree of aggregation, which rendered DLS measurements non-viable.

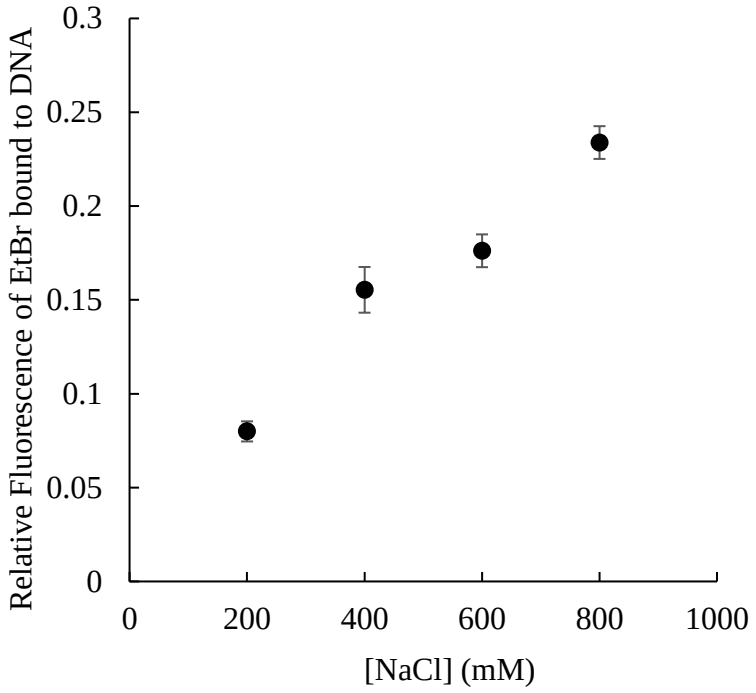

Figure 4.9. Effect of ionic concentration on DNA drug binding in the presence of PEI. Data representative of n=3. Data determined to be statistically significant through One-way Anova testing. Fluorescence is relative to the maximum amount of fluorescence exhibited by EtBr when in the presence of DNA.

Furthermore, varying charge ratios were used to determine the capability of drug binding to DNA with respect to the presence of cations (Figure 4.10). Again, EtBr was used as the drug of interest to determine the limitations of increasing PEI concentration. At low charge ratios (PEI Primary Amines: DNA Backbone Phosphates), EtBr was successfully bound to DNA allowing for high fluorescence detection. Specifically, with a ten-fold increase to the charge ratio, the higher strength of condensation to the PEI surface decreased the binding of EtBr by 61%.

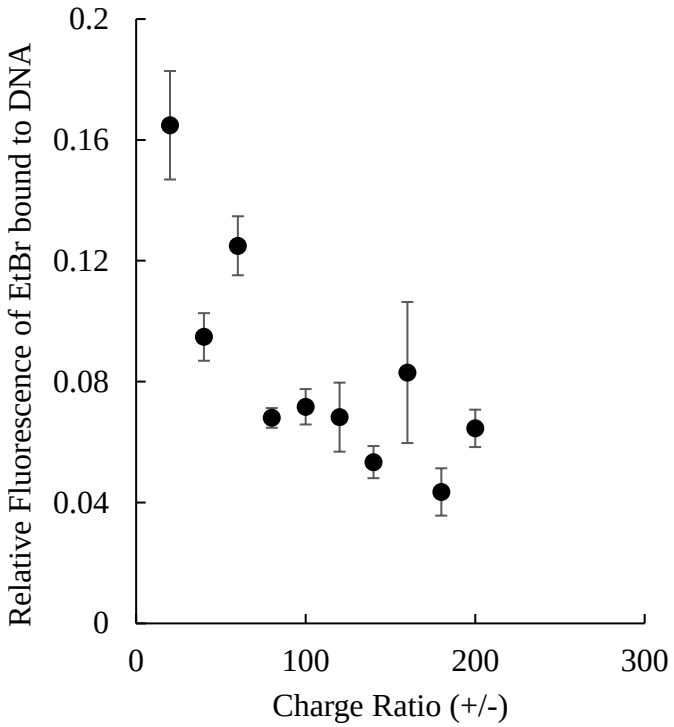

Figure 4.10. Effect of charge ratio on DNA drug binding in the presence of PEI. Data representative of n=3. Data determined to be statistically significant through One-way Anova testing. Charge ratios were calculated using FTIR analysis to determine the absorbance of primary amines as compared to the backbone phosphates of PEI. Fluorescence is relative to the maximum amount of fluorescence exhibited by EtBr when in the presence of DNA.

4.3 Comparison of Drug Loading Methods

To determine the extent to which PEI binding inhibits the ability of DNA-Daun complex formation, gel electrophoresis was used. By loading daunorubicin to DNA at two separate points during synthesis, either before or simultaneously in addition to HCPPs, we distinguished the differences in mass of drug loaded per particle. DNA loaded prior to addition to PEI nanoparticles can load a higher volume of drug than PEI-DNA conjugates are formed (Figure 4.11). With equivalent charge and morphologies, the only contribution to the decrease in band traveling would be the mass of the particles. There was a statistically

significant 32% decrease in the total drug mass loaded when drug was loaded with DNA simultaneously (Figure A3). This implies that the binding of the DNA backbone to PEI free amines results in a decrease in DNA intercalating daunorubicin. This upholds our current understanding of the interactions between intercalative drug and cationic polymer nanocarriers.[161] Previous results from the charge ratio analysis (Figure 4.10) also corroborate this, as the presence of cations shows a decrease in the ability of DNA to bind another intercalative drug.

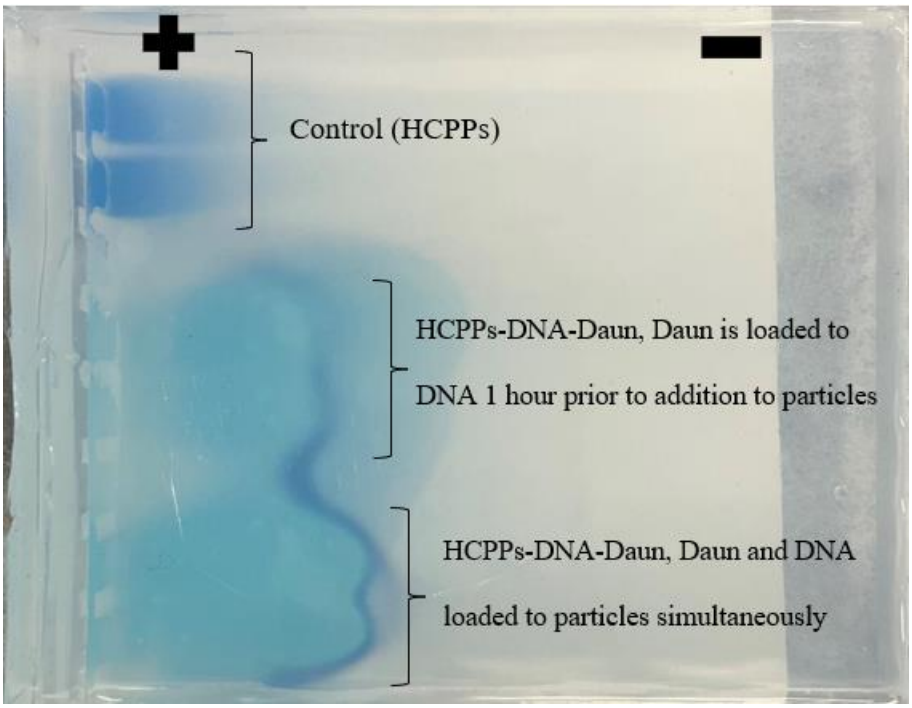

Figure 4.11. Gel electrophoresis for determination of density of drug loading. Copper addition was used to create the blue Cu-PEI complex, allowing for facile observation of bands by the naked eye. Differences in morphology and zeta potential were determined to be insignificant through DLS and Zetasizer measurements.

Chapter 5

Drug Loading and Release

5.1 Daunorubicin Affinity Towards the Chosen Set of DNA Sequences

To understand the loading and release mechanism of daunorubicin within our synthesized platform, we must first understand the innerworkings of daunorubicin's binding to DNA. To do this, we studied the potential of daunorubicin binding with increasing concentration (Figure 5.1). As anticipated, increasing the molar concentration of daunorubicin in relation to the molar concentration of DNA in solution increased the total amount of drug bound per strand of DNA. There was a clear linear relationship found between the increase in daunorubicin in solution, and the total amount bound to the nucleic acid. The different compositions of strands did not show any significant difference in binding. Strands with a longer length on average showed a higher number of molecules bound per strand of DNA in solution. This corroborates the evidence that there is a higher number of binding sites on strands of a longer length.[162] At higher concentrations of daunorubicin (Daun: DNA concentration ratio ≥500), this difference was negligible.

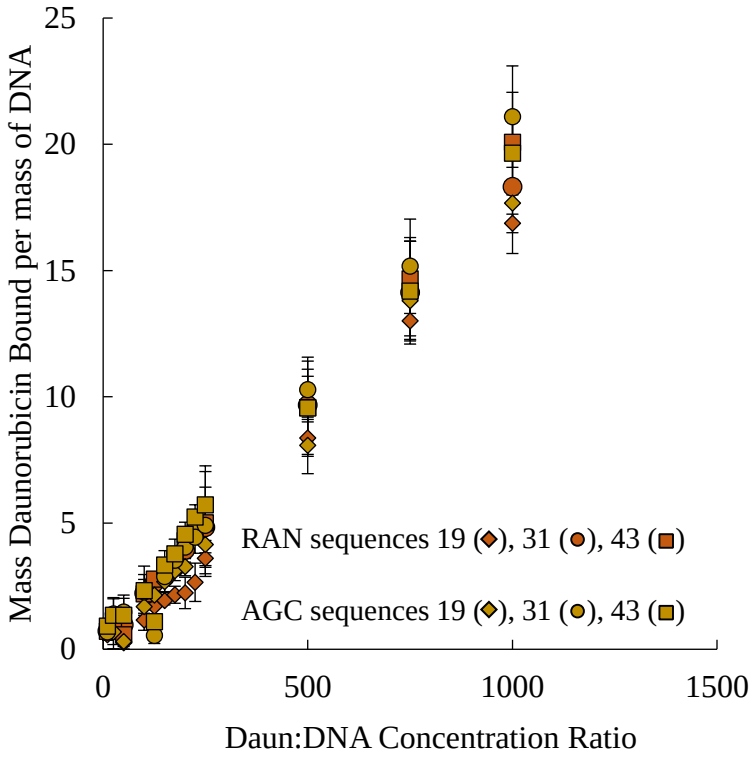

Figure 5.1. Mass of daunorubicin bound per mass of DNA. RAN sequences 19 (◆), 31 (●), 43 (■) and AGC sequences 19 (◆), 31 (●), 43 (■) were compared on Hollow Core PEI Nanoparticles loaded with daunorubicin. Data is representative of n=3. DNA concentration of 2 µM was used consistently.

Through these results, the dissociation constants (Table 5.1) and Hill Coefficients were calculated. The dissociation constant (Kd) describes the rate at which the ligand detaches itself from the protein in comparison to the rate at which the protein-ligand complex forms. A lower dissociation constant indicates higher affinity towards the formation of a complex between DNA and daunorubicin. Dissociation constants between the range of 10^{-9}—10^{-12} M are a high affinity towards the formation of complex formation.[163] All sequences were determined to have a moderately high affinity towards the formation of the complex, with no significant differences in affinity between the different strand compositions. There was a trend observed in that as the length of the strand increased, there was an increase in the

affinity towards binding. This further indicates that increasing the number of available binding sites increases the ability of daunorubicin to intercalate to the DNA nucleotides.

Table 5.1

Dissociation Constants of DNA-Daun Complex

	Dissociation Constant (nM)	
RAN-19	RAN-31	RAN-43
7.24 +/- 0.31	4.37 +/- 0.57	0.548 +/- 0.55
AGC-19	AGC-31	AGC-43
12.02 +/- 0.36	7.41 +/- 0.35	1.48 +/- 0.49

Note. Dissociation constants are calculated under the assumption that daunorubicin requires 3 nucleotides to bind. Deviation is determined through comparison of linear regression models.

Furthermore, an analysis of the Hill Coefficients (n) shows that cooperativity in binding becomes more positive as the length of the strand increases (Table 5.2). This denotes that daunorubicin binding further promotes additional drug intercalation. This validates previous studies into the binding functionality of daunorubicin to DNA.[164]

Table 5.2.

DNA-Daun Complex Hill Coefficients

	Hill Coefficients	
RAN-19	RAN-31	RAN-43
1.0299	1.0748	1.4491
AGC-19	AGC-31	AGC-43
0.9528	0.939	1.2534

Note. Hill Coefficients (n) were calculated for each DNA sequence. Hill coefficients n >1 indicate cooperative binding. A Hill Coefficient less than 1 is associated with negative cooperativity, indicating that daunorubicin binding inhibits further binding of daunorubicin.

5.2 Release Profile of Daunorubicin

The key metric to understand the viability of our platform as a drug delivery vehicle is to ascertain the profile of release from the hollow core with DNA structure as compared to both unbound daunorubicin as well as drug loaded to the interior of a hollow core nanoparticle. Our tests were conducted until it was verified that all mass released was calculated. All release studies were conducted in PBS to mimic biological conditions.[165]

5.2.1 Release from HCPPs-DNA-Daun

The fractional releases of all strands were compared to contrast the profile and rate of release from the Hollow Core PEI Nanoparticles (Figure 5.2). All strands maintained an extended release over a 12-hour period following Peppas-Korsmeyer modeling. All constants are representative of Fickian diffusion for spherical samples ($n<0.43$). This leads us to believe that the primary factor driving drug release is concentration driven separation from the DNA followed by the diffusion of the encapsulated drug through the polymeric layer. The profiles in the release show no trends in terms of strand composition. This upholds the previous assertion that there is trivial difference in dissociation between strand

composition. Additionally, there is no trend in terms of strand length, further justifying the idea that there are no significant differences in the dissociation profile of the DNA-Daun complex in terms of strand length or the number of available binding sites.

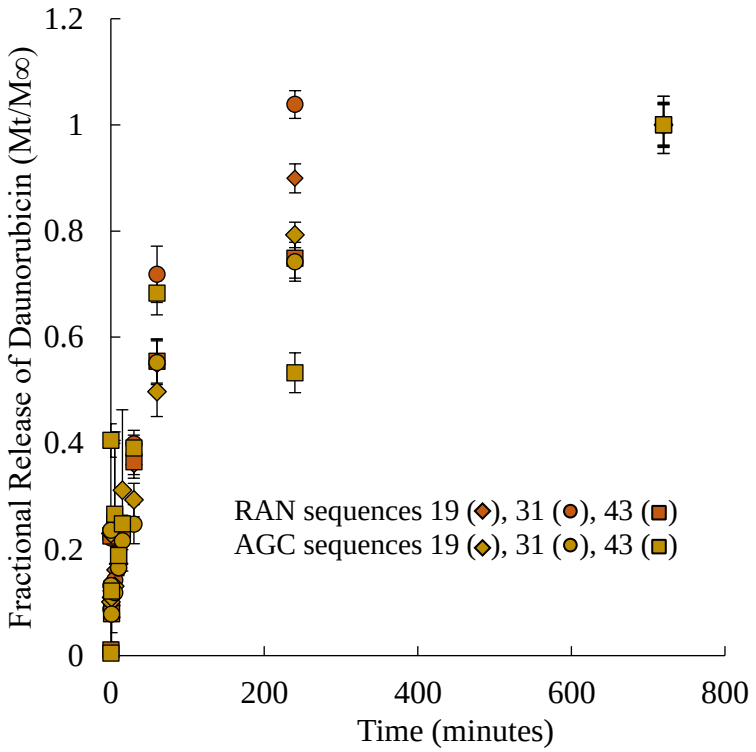

Figure 5.2. Fractional release of daunorubicin from HCPPs-DNA-Daun. RAN sequences 19 (◆), 31 (●), 43 (■) and AGC sequences 19 (◆), 31 (●), 43 (■) were compared on Hollow Core PEI Nanoparticles loaded with daunorubicin. Data is representative of n=3.

The cumulative mass release for all strands were compared by length to determine differences in mass release and loading. Particles were grouped by strand compositions random sequences (Figure 5.3A) and the designer AGC sequences (Figure 5.3B), with all lengths represented. Strands with the longest sequence length on average released 8.75 ± 0.25 mg more than their smallest counterparts. This further validates the understanding that

longer sequences contain more sites for drug binding. Though the total mass loaded was increased for longer strands, the profile of release remained consistent between strand lengths. The AGC strands on average released a total of 3.83 ± 0.33 mg more than their RAN counterparts.

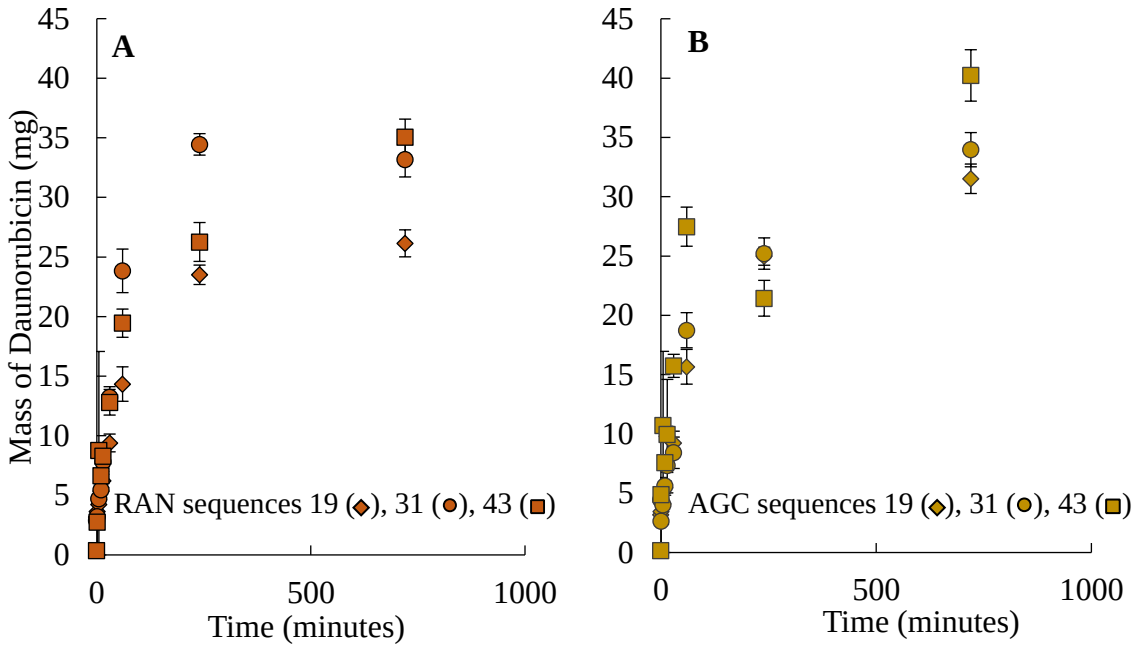

Figure 5.3. Daunorubicin mass release of HCPPs-DNA-Daun. RAN sequences (A) 19 (◆), 31 (●), 43 (■) and AGC sequences (B) 19 (◆), 31 (●), 43 (■) were compared on Hollow Core PEI Nanoparticles loaded with daunorubicin. Data is representative of n=3.

5.2.2 Release from PEI-X-AuNP-DNA-Daun

To evaluate the drug release of HCPPs, the fractional mass release of solid core particles was compared (Figure 5.4). When observing the fractional release of the PEI-X-AuNP-DNA-Daun, the total time to release the entirety of the payload is reduced to 1 hour as compared to the 12-hour release seen in HCPPs-DNA-Daun. The longer time required to release in the HCPPs could be indicative of the ability of the hollow sphere to retain

drug and release over a slower period. This can be better seen when comparing mass release where HCPPs can load a much higher mass of drug (Figure 5.5). The hollow core particles were able to load 225 ± 44.6mg more drug per cm^3 of nanoparticles than the solid core formulation. This change in drug loading capability is hypothesized to be attributed to the hollow morphology as the differences in DNA able to be loaded to both are not statistically significant. This is further supported by analyzing the differences in available volume for each particle, compared to the total amount of drug volume loaded (Figure A4). Another possibility is that the hollow surface does not disrupt the ability of the daunorubicin to load as greatly as a solid surface would. Release orders of the fractional release were calculated to determine the mechanisms of release (Table 5.3). Potential sources of error include possible photobleaching of daunorubicin when exposed to light for extended periods. Additionally, daunorubicin is not detectable at low concentrations as the hydrophobic molecule moves to the edge of the well plate. This may have resulted in lower values of fluorescence that did not represent the actual amount of daunorubicin released.

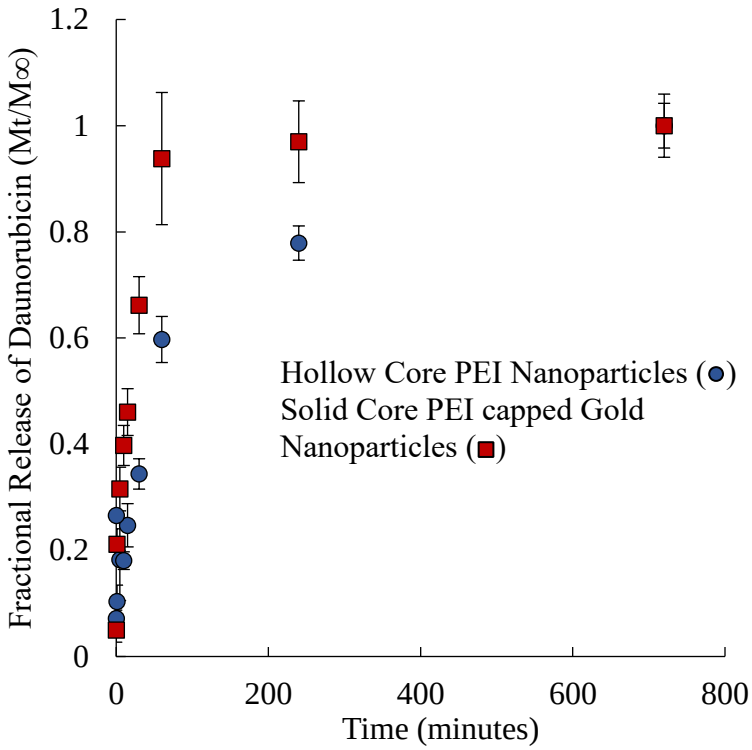

Figure 5.4. Fractional release of daunorubicin from hollow and solid core polyethyleneimine nanoparticles with DNA-Daun. Fractional release of Hollow Core PEI Nanoparticles Conjugated to DNA loaded with daunorubicin (●) were compared to Solid Core PEI capped Gold Nanoparticles conjugated with DNA loaded with daunorubicin (■). Data is representative of n=3. All DNA strands were aggregated.

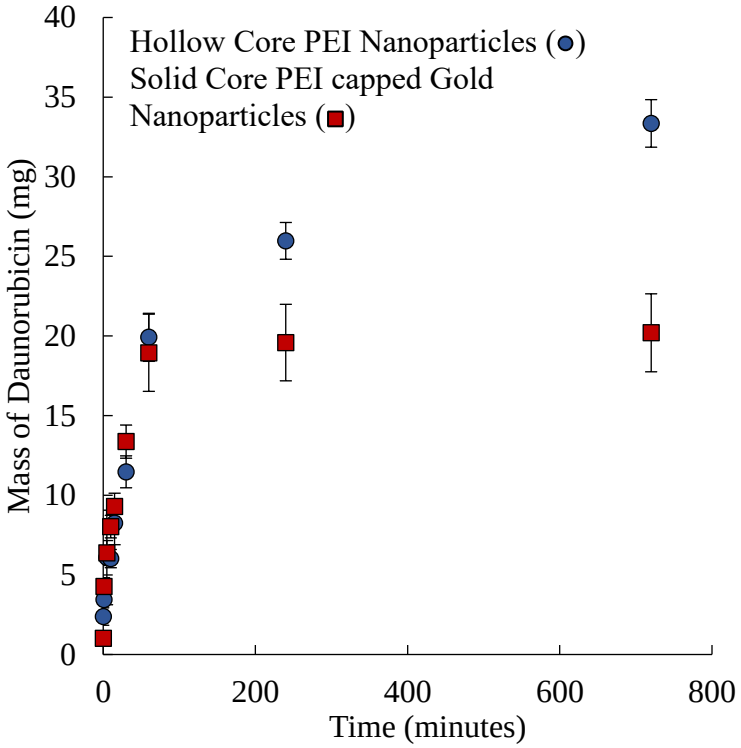

Figure 5.5. Mass release of daunorubicin from hollow and solid core polyethyleneimine nanoparticles with DNA-Daun. Total mass release of Hollow Core PEI Nanoparticles Conjugated to DNA loaded with daunorubicin (●) were compared to Solid Core PEI capped Gold Nanoparticles conjugated with DNA loaded with daunorubicin (■). Data is representative of n=3. All DNA strands were aggregated.

Table 5.3

Order of Daunorubicin Release for Solid and Hollow Core Particles

	RAN-19	AGC-19	RAN-31	AGC-31	RAN-43	AGC-43
Solid Particles	0.41	0.17	0.16	0.16	0.19	0.22
Hollow Particles	0.35	0.37	0.42	0.42	0.37	0.30

Note. The order of daunorubicin release from the particles were compared for solid particles (AuNP-PEI-DNA-Daun) and hollow particles (PEI-DNA-Daun). The order number (n) is calculated as the value in the release equation $Mt/M\infty=k*t^n$ where M_t is the mass released at a given timepoint, $M\infty$ is the mass released as time approaches infinity, k is a release constant, and "t" is time. The "n" value is considered valid up to the first 60% of mass release.

5.4 Assessment of DNA Stability

5.4.1 Nuclease Degradation

The effects on particle bound DNA drug loading capability by DNA degrading nuclease were determined through comparison to the effects on DNA suspended in buffer (Figure 5.6). HCPPs were shown to mitigate the degradation of DNA when bound to the surface in contrast to DNA left to degrade in buffer. EtBr was again used as an intercalative agent to determine if DNA remained capable of binding drug between base pairs. This would be impossible if the backbone of the DNA were eroded through nuclease degradation. Solid core gold nanoparticles were able to inhibit the degradation of the DNA backbone, exhibiting a 46% reduction in binding functionality after 10 minutes of exposure. HCPPs were shown to limit degradation of functional DNA to an average of 32%, whereas DNA simply suspended had a reduction in functional binding of 62%. This corresponds to the protective effects on DNA when bound to the surfaces of PEI nanoparticles. The strong electrostatic bonds between these molecules limit the

effectiveness of DNAse by sterically hindering their interactions. DNA loaded on PEI particles will be more likely to retain its drug loading function when exposed to the nucleases present in lysosomes.[166] Hollow core PEI particles are also more effective than solid core gold nanoparticles in protecting nucleic acid. This further indicates a difference in DNA morphology on the surface. Nuclease targets the exposed backbone on the gold particle and is less effective in targeting the condensed backbone on the PEI particle surface. This is important for DNA drug delivery, as foreign DNA will naturally provoke immune response *in vivo*. This finding shows that HCPPs are better DNA drug delivery vectors will be more stable when delivering drug loaded DNA which may lead to more effective drug delivery.

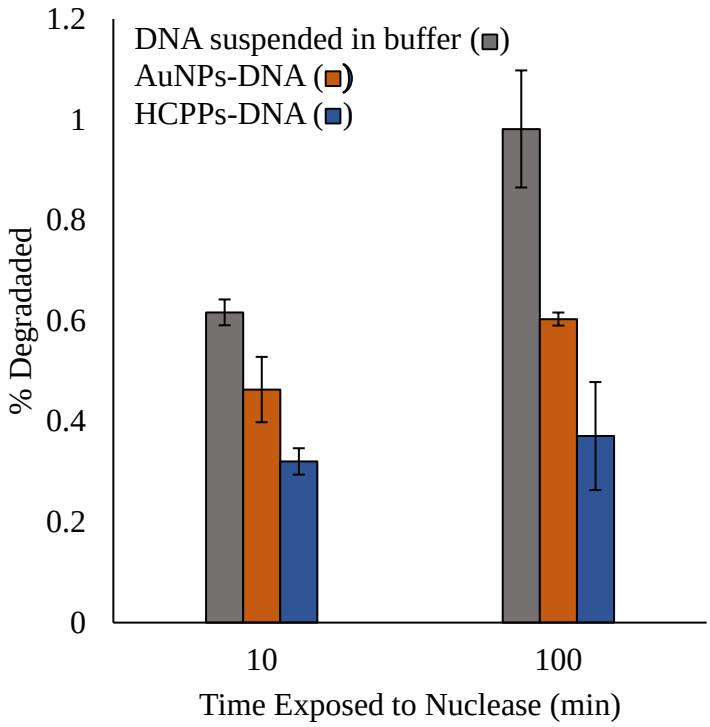

Figure 5.6. Stability of DNA when exposed to nuclease. DNA suspended in buffer (■), Gold nanoparticles with DNA (■), and Hollow core PEI nanoparticles conjugated with DNA (■) were compared for nuclease degradation. Samples were incubated with 0.0717 units of DNAse I for 10 minutes before the reaction was stopped using Tris-EDTA buffer. After introduction of a base to shift to pH 9 and 48 hours of incubation, the fluorescence of EtBr was checked to ascertain the remaining concentration of functional DNA. Values calculated as a percentage of the remaining EtBr fluorescence following nuclease degradation, in relation to the total EtBr fluorescence shown prior to DNAse introduction. EtBr suspended in water was used as a baseline. Data is representative of n=3.

5.4.2 Particle Stability in Albumin

The effects of suspending particles in albumin were determined through dynamic light scattering analysis (Figure 5.7). The diameter of particles suspended in buffer were compared to those in albumin to assess particle aggregation and stability. There was no statistical significance found in particle diameter between the buffer suspended and albumin suspended particles. This indicates that particles do not aggregate in the presence of albumin, nor bind many proteins to the surface. Thus, we hypothesize that these particles

would remain stable within the bloodstream. This is a key functionality of the delivery system which would allow it to be viable in a clinical setting.

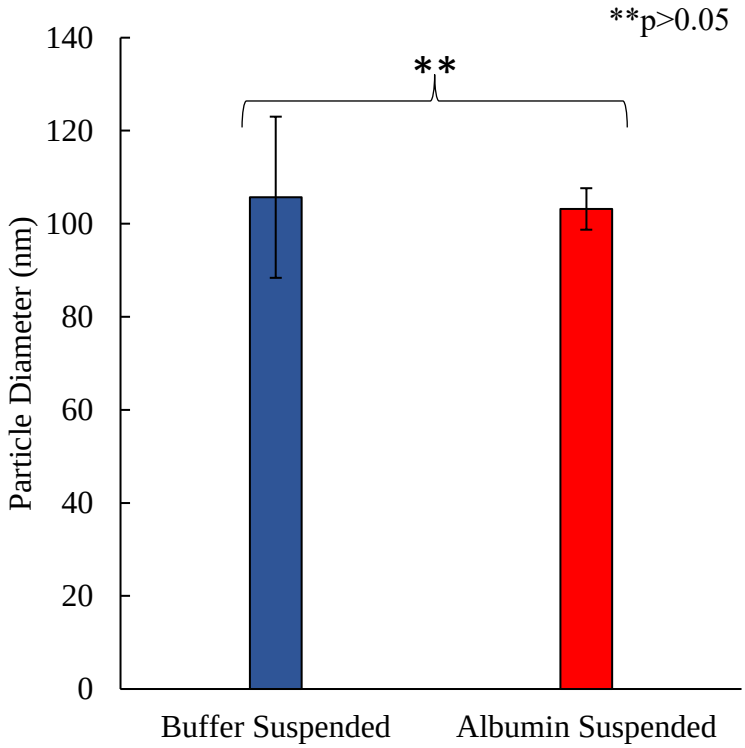

Figure 5.7. Hollow core particle diameter when suspended in buffer versus albumin. HCPPs-DNA-Daun were suspended in either Tris-EDTA pH 8.0 (■) or 10 mg/mL of bovine serum albumin (■). Samples were tested for diameter through DLS measurement 1 hour after suspension at 37°C. Significance was determined through One-way Anova testing. Data is representative of n=3.

Chapter 6

Conclusions and Future Work

6.1 Conclusions

Cancer treatments are highly limited in their ability to extend the release of payloads and protect those payloads from the surrounding environment. Nanoparticles have been used in recent years to combat the disadvantages of modern cancer treatment. Further augmentation of the nanoparticles can be conducted through the addition of polymers, which enhance the nanoparticle physical and chemical properties for drug delivery purposes. Nucleic acids have been employed recently as efficient drug carriers due to their ability to intercalate chemotherapeutic drug daunorubicin. Hollow core nanoparticles were further used to increase the drug payload and protect nucleic acids from degradation. However, these methods have not been used together for chemotherapeutic drug delivery. In this work, we synthesized novel polyethyleneimine-based hollow nanoparticles from a gold nanoparticle template that can bind both DNA and daunorubicin for chemotherapy. By utilizing well-studied modern techniques, this research was successful in synthesizing and characterizing a novel drug delivery platform.

The physical and chemical characteristics of the particles were well understood. Hollow core polyethyleneimine nanoparticles with electrostatically bound DNA loaded with daunorubicin were found to have a total diameter of 105.7 ± 17.3 nm. This was near the desired target of 100 nm, which allows the particles to enter the tumor microenvironment while avoiding the inherent cytotoxicity of particles below 20 nm. Particle zeta potential was +20.4 ± 3.5 mV, which exceeded the target of +20 mV. The

high zeta potential allows the particle to travel towards the negatively charged cell membrane and limit the amount of aggregation in the particle sample. Particles were determined to have a spherical morphology due to the singular peak detected through DLS measurements. The removal of the gold core was verified by absorbance measurements, which did not display an absorbance at the associated 520 nm peak typical of gold nanoparticles. The particle's composition was further determined through FTIR analysis, which identified a 4:1 ratio of primary to tertiary amines in the particle's PEI.

The capability of the HCPP as a nucleic acid and drug delivery platform were thoroughly investigated. The particle could bind a high density of nucleic acids to the surface, greater than 80 strands per particle. This was lower than the amount bound to a gold nanoparticle surface, indicating an architectural difference in the surface binding of nucleic acids, though a sufficiently high amount of DNA was still bound to the PEI particle surface for high dosage drug delivery. We thus hypothesize that the DNA binds in a toroidal formation, electrostatically binding the backbone to the surface of the HCPPs. Increasing the particle solution's ionic concentration increased the intercalation of drug to the nucleic acid. A 4-fold increase in ionic concentration corresponded with a 64% increase in drug intercalation. Inversely, increasing the charge ratio of PEI amines to the nucleic acid phosphate backbones showed a resultant decrease in the ability to bind drug. A 10-fold increase in the amine: phosphate ratio saw a corresponding 61% decrease in drug intercalation. Furthermore, it was shown that by intercalating daunorubicin to the DNA prior to addition to the nanoparticle, DNA was able to load 32% more drug than if the DNA and daunorubicin are added to the particle in tandem.

The release of drug from the platform was well characterized. HCPPs were found to load a total of 225 ± 44.6mg more drug per cm^3, which is significantly higher than the standard 5 mg/mL used in clinical settings.[167] The platform was shown to deliver a higher amount of drug than the solid core formulation, releasing 225 ± 44.6mg more drug per cm^3 of nanoparticles. We hypothesize that this difference in loaded volume is due to the hollow structure which allows for increased loading to the interior. The interior space available for loading was determined to be that of the actual difference in volume noted between the hollow core and solid core formulation. Additionally, the hollow core particle was shown to release an order of magnitude longer than the 1-hour release shown by solid core particle. The platform extends the release of chemotherapeutics, which can decrease the side effects on patients and increase the overall patient quality of life.

Finally, the stability of the particles when exposed to different proteins was assessed. HCPPs were found to limit the degradation of the DNA backbone by nuclease. HCPPs retained the functionality of the DNA backbone 60% more than DNA in solution and 23% more than AuNPs. Furthermore, HCPPs remained stable in the presence of albumin, no aggregation of the particles or surface proteins were observed. This platform is shown to be viable in the presence of several proteins that would be found in *in vivo* conditions. Overall, the HCPPs were shown to be an efficient drug carrier that can successfully protect its payload from surrounding proteins. This drug delivery vessel has potential to increase the effectiveness of chemotherapeutic treatment and be used as a precedent for developing novel nanomaterials.

6.2 Future Work

Monitoring the interactions between the HCPPs-Daun-DNA particles and living cells is important for progress towards clinical use of these vehicles for drug delivery. *In vitro* cell studies would be a critical first step in determining how effective this platform would be in a clinical setting. Future work should include studies focusing on the ability of the nanoparticle platform to cross the membrane of tumor cells in a specific cell line. Analyzing the drug's ability to leave the associated endosome would be key in determining the nanostructure's efficiency as a drug delivery vessel. Furthermore, the addition of a targeting ligand would increase the efficiency of nanoparticle delivery to the desired tumor site, thus improving therapeutic outcomes. Creating a facile synthesis process for a clinically used ligand would be a vital next phase in designing an effective drug carrier. The investigation into the cell transport and endosomal escape between the HCPPs-Daun-DNA within carcinogenic tissue would supply a clear indication of the need for our synthesized system.

References

1. Mariotto AB, Enewold L, Zhao J, Zeruto CA, Yabroff KR. Medical Care Costs Associated with Cancer Survivorship in the United States. *Cancer Epidemiol Biomarkers Prev*. 2020;29(7):1304-1312. doi:10.1158/1055-9965.EPI-19-1534

2. Arruebo M, Vilaboa N, Sáez-Gutierrez B, et al. Assessment of the Evolution of Cancer Treatment Therapies. *Cancers* . 2011;3(3). doi:10.3390/cancers3033279

3. Winters-Stone KM, Horak F, Jacobs PG, et al. Falls, Functioning, and Disability Among Women With Persistent Symptoms of Chemotherapy-Induced Peripheral Neuropathy. *J Clin Oncol*. 2017;35(23):2604-2612. doi:10.1200/JCO.2016.71.3552

4. Zugazagoitia J, Guedes C, Ponce S, Ferrer I, Molina-Pinelo S, Paz-Ares L. Current Challenges in Cancer Treatment. *Clin Ther*. 2016;38(7):1551-1566. doi:https://doi.org/10.1016/j.clinthera.2016.03.026

5. Pucci C, Martinelli C, Ciofani G. Innovative approaches for cancer treatment: current perspectives and new challenges. *Ecancermedicalscience*. 2019;13:961. doi:10.3332/ecancer.2019.961

6. Wu H, Chang D, Huang C. Targeted Therapy for Cancer. 2014;(January 2006).

7. Lee YT, Tan YJ, Oon CE. Molecular targeted therapy: Treating cancer with specificity. *Eur J Pharmacol*. 2018;834:188-196. doi:https://doi.org/10.1016/j.ejphar.2018.07.034

8. Ke X, Shen L. Molecular targeted therapy of cancer: The progress and future prospect. *Front Lab Med*. 2017;1(2):69-75. doi:https://doi.org/10.1016/j.flm.2017.06.001

9. Yao Y, Zhou Y, Liu L, et al. Nanoparticle-Based Drug Delivery in Cancer Therapy and Its Role in Overcoming Drug Resistance . *Front Mol Biosci* . 2020;7. https://www.frontiersin.org/article/10.3389/fmolb.2020.00193

10. Kreuter J. Nanoparticles—a historical perspective. *Int J Pharm*. 2007;331(1):1-10. doi:https://doi.org/10.1016/j.ijpharm.2006.10.021

11. Roth MT, Cardin DB, Berlin JD. Recent advances in the treatment of pancreatic cancer. *F1000Research*. 2020;9:F1000 Faculty Rev-131. doi:10.12688/f1000research.21981.1

12. Guo D, Xie G, Luo J. Mechanical properties of nanoparticles: basics and applications. *J Phys D Appl Phys*. 2013;47(1):13001. doi:10.1088/0022-3727/47/1/013001

13. Han X, Xu K, Taratula O, Farsad K. Applications of nanoparticles in biomedical imaging. *Nanoscale*. 2019;11(3):799-819. doi:10.1039/c8nr07769j

14. Wolfram J, Zhu M, Yang Y, et al. Safety of Nanoparticles in Medicine. *Curr Drug Targets*. 2015;16(14):1671-1681. doi:10.2174/1389450115666140804124808

15. Ferrari M. Frontiers in cancer nanomedicine: directing mass transport through biological barriers. *Trends Biotechnol*. 2010;28(4):181-188. doi:https://doi.org/10.1016/j.tibtech.2009.12.007

16. La-Beck NM, Gabizon AA. Nanoparticle Interactions with the Immune System: Clinical Implications for Liposome-Based Cancer Chemotherapy . *Front Immunol* . 2017;8. https://www.frontiersin.org/articles/10.3389/fimmu.2017.00416

17. Medina C, Santos-Martinez MJ, Radomski A, Corrigan OI, Radomski MW. Nanoparticles: pharmacological and toxicological significance. *Br J Pharmacol*. 2007;150(5):552-558. doi:10.1038/sj.bjp.0707130

18. Mody V V, Siwale R, Singh A, Mody HR. Introduction to metallic nanoparticles. *J Pharm Bioallied Sci*. 2010;2(4):282-289. doi:10.4103/0975-7406.72127

19. Phan HT, Haes AJ. What Does Nanoparticle Stability Mean? *J Phys Chem C*. 2019;123(27):16495-16507. doi:10.1021/acs.jpcc.9b00913

20. Praetorius NP, Mandal TK. Engineered Nanoparticles in Cancer Therapy Engineered Nanoparticles in Cancer Therapy. 2014;(February 2007). doi:10.2174/187221107779814104

21. Moghimi SM, Hunter AC, Murray JC. Nanomedicine : current status and future prospects. doi:10.1096/fj.04-2747rev

22. Wang AZ, Langer R, Farokhzad OC. Nanoparticle Delivery of Cancer Drugs. *Annu Rev Med*. 2012;63(1):185-198. doi:10.1146/annurev-med-040210-162544

23. Sun T, Zhang YS, Pang B, Hyun DC, Yang M. Y. Xia Engineered nanoparticles for drug delivery in cancer therapy Angew. *Chem Int Ed*. 2014;53:12320-12364.

24. Lim Z-ZJ, Li J-EJ, Ng C-T, Yung L-YL, Bay B-H. Gold nanoparticles in cancer therapy. *Acta Pharmacol Sin*. 2011;32(8):983-990. doi:10.1038/aps.2011.82

25. Siddique S, Chow JCL. applied sciences Gold Nanoparticles for Drug Delivery and Cancer Therapy. Published online 2020.

26. Peng J, Liang X. Progress in research on gold nanoparticles in cancer management. *Medicine (Baltimore)*. 2019;98(18):e15311. doi:10.1097/MD.0000000000015311

27. Singh P, Pandit S, Mokkapati VRSS, Garg A, Ravikumar V, Mijakovic I. Gold Nanoparticles in Diagnostics and Therapeutics for Human Cancer. *Int J Mol Sci*. 2018;19(7):1979. doi:10.3390/ijms19071979

28. Kadkhoda J, Aghanejad A, Safari B, Barar J, Rasta SH, Davaran S. Aptamer-conjugated gold nanoparticles for targeted paclitaxel delivery and photothermal therapy in breast cancer. *J Drug Deliv Sci Technol*. 2022;67:102954. doi:https://doi.org/10.1016/j.jddst.2021.102954

29. Finkelsteint AE, Walz DT, Batista V, Mizraji M, Roisman F, Misher A. Auranofin * New oral gold compound for treatment of rheumatoid arthritis. 1976;39162:251-257.

30. Unfried K, Albrecht C, Klotz L-O, Von Mikecz A, Grether-Beck S, Schins RPF. Cellular responses to nanoparticles: Target structures and mechanisms. *Nanotoxicology*. 2007;1(1):52-71. doi:10.1080/00222930701314932

31. Chen Y-S, Hung Y-C, Liau I, Huang GS. Assessment of the In Vivo Toxicity of Gold Nanoparticles. *Nanoscale Res Lett*. 2009;4(8):858. doi:10.1007/s11671-009-9334-6

32. Dobrovolskaia MA, Aggarwal P, Hall JB, McNeil SE. Preclinical studies to understand nanoparticle interaction with the immune system and its potential effects on nanoparticle biodistribution. *Mol Pharm*. 2008;5(4):487-495. doi:10.1021/mp800032f

33. Dobrovolskaia MA, Patri AK, Zheng J, et al. Interaction of colloidal gold nanoparticles with human blood: effects on particle size and analysis of plasma protein binding profiles. *Nanomedicine*. 2009;5(2):106-117. doi:10.1016/j.nano.2008.08.001

34. Ostrowski AD, Martin T, Conti J, Hurt I, Harthorn BH. Nanotoxicology: characterizing the scientific literature, 2000–2007. *J Nanoparticle Res*. 2009;11(2):251-257. doi:10.1007/s11051-008-9579-5

35. Alkilany AM, Murphy CJ. Toxicity and cellular uptake of gold nanoparticles: what we have learned so far? *J nanoparticle Res an Interdiscip forum nanoscale Sci Technol*. 2010;12(7):2313-2333. doi:10.1007/s11051-010-9911-8

36. Chan JM, Valencia PM, Zhang L, Langer R, Farokhzad OC. Chapter 11 Polymeric Nanoparticles for Drug Delivery. :163-175. doi:10.1007/978-1-60761-609-2

37. Soppimath KS, Aminabhavi TM, Kulkarni AR, Rudzinski WE. Biodegradable polymeric nanoparticles as drug delivery devices. *J Control Release*. 2001;70(1):1-20. doi:https://doi.org/10.1016/S0168-3659(00)00339-4

38. des Rieux A, Fievez V, Garinot M, Schneider Y-J, Préat V. Nanoparticles as potential oral delivery systems of proteins and vaccines: A mechanistic approach. *J Control Release*. 2006;116(1):1-27. doi:https://doi.org/10.1016/j.jconrel.2006.08.013

39. Kumari A, Yadav SK, Yadav SC. Biodegradable polymeric nanoparticles based drug delivery systems. *Colloids Surfaces B Biointerfaces*. 2010;75(1):1-18. doi:https://doi.org/10.1016/j.colsurfb.2009.09.001

40. Shah M, Naseer MI, Choi MH, Kim MO, Yoon SC. Amphiphilic PHA–mPEG copolymeric nanocontainers for drug delivery: Preparation, characterization and in vitro evaluation. *Int J Pharm*. 2010;400(1):165-175. doi:https://doi.org/10.1016/j.ijpharm.2010.08.008

41. Masood F. Polymeric nanoparticles for targeted drug delivery system for cancer therapy. *Mater Sci Eng C*. 2016;60:569-578. doi:https://doi.org/10.1016/j.msec.2015.11.067

42. Brewer E, Coleman J, Lowman A. Emerging Technologies of Polymeric Nanoparticles in Cancer Drug Delivery. Sun L, ed. *J Nanomater*. 2011;2011:408675. doi:10.1155/2011/408675

43. Parveen S, Sahoo SK. Polymeric nanoparticles for cancer therapy. 2008;2330. doi:10.1080/10611860701794353

44. He Y, Cheng G, Xie L, Nie Y, He B, Gu Z. Polyethyleneimine/DNA polyplexes with reduction-sensitive hyaluronic acid derivatives shielding for targeted gene delivery. *Biomaterials*. 2013;34(4):1235-1245. doi:10.1016/j.biomaterials.2012.09.049

45. Zhonghui C, Lv Z. Recent advancements in polyethyleneimine-based materials and their biomedical, biotechnology, and biomaterial applications. 2020;(March). doi:10.1039/C9TB02271F

46. Norouzi P, Motasadizadeh H, Atyabi F, et al. Combination Therapy of Breast Cancer by Codelivery of Doxorubicin and Survivin siRNA Using Polyethylenimine Modified Silk Fibroin Nanoparticles. *ACS Biomater Sci Eng*. 2021;7(3):1074-1087. doi:10.1021/acsbiomaterials.0c01511

47. Amjad MW, Amin MCIM, Katas H, Butt AM, Kesharwani P, Iyer AK. In Vivo Antitumor Activity of Folate-Conjugated Cholic Acid-Polyethylenimine Micelles for the Codelivery of Doxorubicin and siRNA to Colorectal Adenocarcinomas. *Mol Pharm*. 2015;12(12):4247-4258. doi:10.1021/acs.molpharmaceut.5b00827

48. Dong D-W, Tong S-W, Qi X-R. Comparative studies of polyethylenimine–doxorubicin conjugates with pH-sensitive and pH-insensitive linkers. *J Biomed Mater Res Part A*. 2013;101A(5):1336-1344. doi:https://doi.org/10.1002/jbm.a.34450

49. Zhang Y, Wei C, Lv F, Liu T. Real-time imaging tracking of a dual-fluorescent drug delivery system based on doxorubicin-loaded globin- polyethylenimine nanoparticles for visible tumor therapy. *Colloids Surfaces B Biointerfaces*. 2018;170:163-171. doi:https://doi.org/10.1016/j.colsurfb.2018.06.008

50. Liu C, Liu F, Feng L, Li M, Zhang J, Zhang N. The targeted co-delivery of DNA and doxorubicin to tumor cells via multifunctional PEI-PEG based nanoparticles. *Biomaterials*. 2013;34(10):2547-2564. doi:https://doi.org/10.1016/j.biomaterials.2012.12.038

51. Patel AG, Kaufmann SH. How does doxorubicin work? *Elife*. 2012;1:e00387. doi:10.7554/eLife.00387

52. Lan S, Xie W, Wang J. PEGylated polyethylenimine-stabilized polypyrrole nanoparticles loaded with DOX for chemo-photothermal therapy of cancer cells PEGylated polyethylenimine-stabilized polypyrrole nanoparticles loaded with DOX for chemo-photothermal therapy of cancer cells. 2019;(August). doi:10.1007/s11051-018-4418-9

53. Kazemi M, Parhizkar E, Samani SM, et al. Targeted co-delivery of paclitaxel and anti P-gp shRNA by low molecular weight PEI decorated with L-3,4-dihydroxyphenylalanine. *Biotechnol Prog*. 2022;n/a(n/a):e3310. doi:https://doi.org/10.1002/btpr.3310

54. Lü J-M, Liang Z, Liu D, Zhan B, Yao Q, Chen C. Two Antibody-Guided Lactic-co-Glycolic Acid-Polyethylenimine (LGA-PEI) Nanoparticle Delivery Systems for Therapeutic Nucleic Acids. *Pharmaceuticals*. 2021;14(9). doi:10.3390/ph14090841

55. Mousazadeh H, Bonabi E, Zarghami N. Stimulus-responsive drug/gene delivery system based on polyethylenimine cyclodextrin nanoparticles for potential cancer therapy. *Carbohydr Polym*. 2022;276:118747. doi:https://doi.org/10.1016/j.carbpol.2021.118747

56. Vitale F, Vitaliano R, Battocchio C, et al. Synthesis and characterization of gold nanoparticles stabilized by palladium(II) phosphine thiol. *J Organomet Chem*. 2008;693(6):1043-1048. doi:https://doi.org/10.1016/j.jorganchem.2007.12.024

57. Tian F, Klabunde KJ. Nonaqueous gold colloids . Investigations of deposition and Ðlm growth on organically modiÐed substrates and trapping of molecular gold clusters with an alkyl amine ¤. Published online 1998:1275-1283.

58. Hostetler MJ, Zhong C-J, Yen BKH, et al. Stable, Monolayer-Protected Metal Alloy Clusters. *J Am Chem Soc*. 1998;120(36):9396-9397. doi:10.1021/ja981454n

59. Rahimi M, Wadajkar A, Subramanian K, et al. In vitro evaluation of novel polymer-coated magnetic nanoparticles for controlled drug delivery. *Nanomedicine Nanotechnology, Biol Med*. 2010;6(5):672-680. doi:https://doi.org/10.1016/j.nano.2010.01.012

60. Fam SY, Chee CF, Yong CY, Ho KL, Mariatulqabtiah AR, Tan WS. Stealth Coating of Nanoparticles in Drug-Delivery Systems. *Nanomater* . 2020;10(4). doi:10.3390/nano10040787

61. Tang H, Guo J, Sun Y, Chang B, Ren Q, Yang W. Facile synthesis of pH sensitive polymer-coated mesoporous silica nanoparticles and their application in drug delivery. *Int J Pharm*. 2011;421(2):388-396. doi:https://doi.org/10.1016/j.ijpharm.2011.10.013

62. Fortuni B, Inose T, Ricci M, et al. Polymeric Engineering of Nanoparticles for Highly Efficient Multifunctional Drug Delivery Systems. *Sci Rep*. 2019;9(1):2666. doi:10.1038/s41598-019-39107-3

63. Bonner DK, Zhao X, Buss H, Langer R, Hammond PT. Crosslinked linear polyethylenimine enhances delivery of DNA to the cytoplasm. *J Control Release*. 2013;167(1):101-107. doi:10.1016/j.jconrel.2012.09.004

64. Rosenkranz AA, Sobolev AS. Polyethylenimine-based polyplex nanoparticles and features of their behavior in cells and tissues. *Russ Chem Bull*. 2015;64(12):2749-2755. doi:10.1007/s11172-015-1220-z

65. Siu YS, Li L, Leung MF, Lee KLD, Li P. Polyethylenimine-Based Amphiphilic Core–Shell Nanoparticles: Study of Gene Delivery and Intracellular Trafficking. *Biointerphases*. 2012;7(1):16. doi:10.1007/s13758-011-0016-4

66. Wang X, Feng J, Bai Y, Zhang Q, Yin Y. Synthesis, Properties, and Applications of Hollow Micro-/Nanostructures. *Chem Rev*. 2016;116(18):10983-11060. doi:10.1021/acs.chemrev.5b00731

67. Lee Y, Lee SH, Kim JS, Maruyama A, Chen X, Park TG. Controlled synthesis of PEI-coated gold nanoparticles using reductive catechol chemistry for siRNA delivery. *J Control Release*. 2011;155(1):3-10. doi:https://doi.org/10.1016/j.jconrel.2010.09.009

68. Cebrián V, Martín-Saavedra F, Yagüe C, Arruebo M, Santamaría J, Vilaboa N. Size-dependent transfection efficiency of PEI-coated gold nanoparticles. *Acta Biomater*. 2011;7(10):3645-3655. doi:https://doi.org/10.1016/j.actbio.2011.06.018

69. Masoumzadeh R, Zare A. Polyethyleneimine - based materials for gene therapy , bioimaging and drug delivery systems applications. 2021;2(1):13-16.

70. Liechty WB, Kryscio DR, Slaughter B V, Peppas NA. Polymers for drug delivery systems. *Annu Rev Chem Biomol Eng*. 2010;1:149-173. doi:10.1146/annurev-chembioeng-073009-100847

71. Gil ES, Hudson SM. Stimuli-reponsive polymers and their bioconjugates. *Prog Polym Sci*. 2004;29(12):1173-1222. doi:https://doi.org/10.1016/j.progpolymsci.2004.08.003

72. Garcı RA. Polyethyleneimine-functionalized large pore ordered silica materials for poorly water-soluble drug delivery. Published online 2014:1437-1447. doi:10.1007/s10853-013-7828-1

73. Arabi S, Javar HA, Khoobi M. Preparation and Characterization of Modified Polyethyleneimine Magnetic Nanoparticles for Cancer Drug Delivery. 2016;2016.

74. Prajapati R, Somoza Á. Albumin Nanostructures for Nucleic Acid Delivery in Cancer: Current Trend, Emerging Issues, and Possible Solutions. *Cancers (Basel)*. 2021;13(14). doi:10.3390/cancers13143454

75. Mdlovu NV, Lin K-S, Chen Y, Wu C-M. Formulation of magnetic nanocomposites for intracellular delivery of micro-RNA for MYCN inhibition in neuroblastoma. *Colloids Surfaces A Physicochem Eng Asp*. 2021;615:126264. doi:https://doi.org/10.1016/j.colsurfa.2021.126264

76. Bauhuber S, Hozsa C, Breunig M, Göpferich A. Delivery of Nucleic Acids via Disulfide-Based Carrier Systems. *Adv Mater*. 2009;21(32-33):3286-3306. doi:https://doi.org/10.1002/adma.200802453

77. Kröhnke C. 8.14 - Polymer Additives. In: Matyjaszewski K, Möller MBT-PSACR, eds. Elsevier; 2012:349-375. doi:https://doi.org/10.1016/B978-0-444-53349-4.00212-0

78. Amirova A, Kirila T, Kurlykin M, Tenkovtsev A, Filippov A. Influence of Cross-Linking Degree on Hydrodynamic Behavior and Stimulus-Sensitivity of Derivatives of Branched Polyethyleneimine. *Polymers (Basel)*. 2020;12(5). doi:10.3390/polym12051085

79. Gosselin MA, Guo W, Lee RJ. Efficient Gene Transfer Using Reversibly Cross-Linked Low Molecular Weight Polyethylenimine. *Bioconjug Chem*. 2001;12(6):989-994. doi:10.1021/bc0100455

80. Meng F, Hennink WE, Zhong Z. Reduction-sensitive polymers and bioconjugates for biomedical applications. *Biomaterials*. 2009;30(12):2180-2198. doi:https://doi.org/10.1016/j.biomaterials.2009.01.026

81. Vinogradov S, Batrakova E, Kabanov A. Poly(ethylene glycol)–polyethyleneimine NanoGel^{TM} particles: novel drug delivery systems for antisense oligonucleotides. *Colloids Surfaces B Biointerfaces*. 1999;16(1):291-304. doi:https://doi.org/10.1016/S0927-7765(99)00080-6

82. Huang T, Zhang L, Chen H, Gao C. A cross-linking graphene oxide–polyethyleneimine hybrid film containing ciprofloxacin: one-step preparation, controlled drug release and antibacterial performance. *J Mater Chem B*. 2015;3(8):1605-1611. doi:10.1039/c4tb01896f

83. Briggs F, Browne D, Asuri P. Role of Polymer Concentration and Crosslinking Density on Release Rates of Small Molecule Drugs. Published online 2022.

84. Breaker RR, Joyce GF. The Expanding View of RNA and DNA Function. *Chem Biol*. 2014;21(9):1059-1065. doi:https://doi.org/10.1016/j.chembiol.2014.07.008

85. Talap J, Zhao J, Shen M, et al. Recent advances in therapeutic nucleic acids and their analytical methods. *J Pharm Biomed Anal*. 2021;206:114368. doi:10.1016/j.jpba.2021.114368

86. Sridharan K, Gogtay NJ. Therapeutic nucleic acids: current clinical status. *Br J Clin Pharmacol*. 2016;82:659-672. doi:10.1111/bcp.12987

87. Tan X, Jia F, Wang P, Zhang K. Nucleic acid-based drug delivery strategies. *J Control Release*. 2020;323:240-252. doi:https://doi.org/10.1016/j.jconrel.2020.03.040

88. Hartmann G. Nucleic Acid Immunity. *Adv Immunol*. 2017;133:121-169. doi:10.1016/bs.ai.2016.11.001

89. Yang W. Nucleases: diversity of structure, function and mechanism. *Q Rev Biophys*. 2011;44(1):1-93. doi:10.1017/S0033583510000181

90. Nguyen J, Szoka FC. Nucleic Acid Delivery: The Missing Pieces of the Puzzle? *Acc Chem Res*. 2012;45(7):1153-1162. doi:10.1021/ar3000162

91. Zhu L, Mahato RI. Lipid and polymeric carrier-mediated nucleic acid delivery. *Expert Opin Drug Deliv*. 2010;7(10):1209-1226. doi:10.1517/17425247.2010.513969

92. Sunshine JC, Bishop CJ, Green JJ. Advances in polymeric and inorganic vectors for nonviral nucleic acid delivery. *Ther Deliv*. 2011;2(4):493-521. doi:10.4155/tde.11.14

93. Piotrowski-Daspit AS, Kauffman AC, Bracaglia LG, Saltzman WM. Polymeric vehicles for nucleic acid delivery. *Adv Drug Deliv Rev*. 2020;156:119-132. doi:https://doi.org/10.1016/j.addr.2020.06.014

94. Lächelt U, Wagner E. Nucleic Acid Therapeutics Using Polyplexes: A Journey of 50 Years (and Beyond). *Chem Rev*. 2015;115(19):11043-11078. doi:10.1021/cr5006793

95. Peng L, Wagner E. Polymeric Carriers for Nucleic Acid Delivery: Current Designs and Future Directions. *Biomacromolecules*. 2019;20(10):3613-3626. doi:10.1021/acs.biomac.9b00999

96. Shenhar R, Rotello VM. Nanoparticles: Scaffolds and Building Blocks. *Acc Chem Res*. 2003;36(7):549-561. doi:10.1021/ar020083j

97. Sun Y, Xia Y. Shape-Controlled Synthesis of Gold and Silver Nanoparticles Author (s): Yugang Sun and Younan Xia Published by : American Association for the Advancement of Science Stable URL : http://www.jstor.org/stable/3833065 . *Am Assoc Adv Sci*. 2011;298(5601):2176-2179.

98. Ding Y, Jiang Z, Saha K, et al. Gold Nanoparticles for Nucleic Acid Delivery. *Mol Ther*. 2014;22(6):1075-1083. doi:https://doi.org/10.1038/mt.2014.30

99. Crew E, Rahman S, Razzak-Jaffar A, et al. MicroRNA Conjugated Gold Nanoparticles and Cell Transfection. *Anal Chem*. 2012;84(1):26-29. doi:10.1021/ac202749p

100. Surapaneni SK, Bashir S, Tikoo K. Gold nanoparticles-induced cytotoxicity in triple negative breast cancer involves different epigenetic alterations depending upon the surface charge. *Sci Rep*. 2018;8(1):12295. doi:10.1038/s41598-018-30541-3

101. Pandey AP, Sawant KK. Polyethylenimine: A versatile, multifunctional non-viral vector for nucleic acid delivery. *Mater Sci Eng C*. 2016;68:904-918. doi:https://doi.org/10.1016/j.msec.2016.07.066

102. Jere D, Jiang HL, Arote R, et al. Degradable polyethylenimines as DNA and small interfering RNA carriers. *Expert Opin Drug Deliv*. 2009;6(8):827-834. doi:10.1517/17425240903029183

103. Vermeulen LMP, De Smedt SC, Remaut K, Braeckmans K. The proton sponge hypothesis: Fable or fact? *Eur J Pharm Biopharm*. 2018;129:184-190. doi:https://doi.org/10.1016/j.ejpb.2018.05.034

104. Wallace KB. Adriamycin-induced interference with cardiac mitochondrial calcium homeostasis. *Cardiovasc Toxicol*. 2007;7(2):101-107. doi:10.1007/s12012-007-0008-2

105. Anselmo AC, Mitragotri S. Nanoparticles in the clinic. *Bioeng Transl Med*. 2016;1(1):10-29. doi:https://doi.org/10.1002/btm2.10003

106. Trieb M, Rauch C, Wellenzohn B, et al. Daunomycin intercalation stabilizes distinct backbone conformations of DNA. *J Biomol Struct Dyn*. 2004;21(5):713-724. doi:10.1080/07391102.2004.10506961

107. Biebricher AS, Heller I, Roijmans RFH, Hoekstra TP, Peterman EJG, Wuite GJL. The impact of DNA intercalators on DNA and DNA-processing enzymes elucidated through force-dependent binding kinetics. *Nat Commun*. 2015;6:7304. doi:10.1038/ncomms8304

108. Zhao Y-X, Shaw A, Zeng X, Benson E, Nyström AM, Högberg B. DNA Origami Delivery System for Cancer Therapy with Tunable Release Properties. *ACS Nano*. 2012;6(10):8684-8691. doi:10.1021/nn3022662

109. Cho Y, Lee JB, Hong J. Controlled release of an anti-cancer drug from DNA structured nano-films. *Sci Rep*. 2014;4(1):4078. doi:10.1038/srep04078

110. Schneider YJ, Baurain R, Zenebergh A, Trouet A. DNA-binding parameters of daunorubicin and doxorubicin in the conditions used for studying the interaction of anthracycline-DNA complexes with cells in vitro. *Cancer Chemother Pharmacol*. 1979;2(1):7-10. doi:10.1007/BF00253097

111. El-Toni AM, Habila MA, Labis JP, et al. Design, synthesis and applications of core–shell, hollow core, and nanorattle multifunctional nanostructures. *Nanoscale*. 2016;8(5):2510-2531. doi:10.1039/c5nr07004j

112. Jang H, Min D-H. Spherically-Clustered Porous Au–Ag Alloy Nanoparticle Prepared by Partial Inhibition of Galvanic Replacement and Its Application for Efficient Multimodal Therapy. *ACS Nano*. 2015;9(3):2696-2703. doi:10.1021/nn506492s

113. Shi Q, Zhang P, Li Y, Xia H, Wang D, Tao X. Synthesis of open-mouthed, yolk–shell Au@AgPd nanoparticles with access to interior surfaces for enhanced electrocatalysis. *Chem Sci*. 2015;6(7):4350-4357. doi:10.1039/c5sc01088h

114. Xie S, Jin M, Tao J, et al. Synthesis and Characterization of Pd@MxCu1−x (M=Au, Pd, and Pt) Nanocages with Porous Walls and a Yolk–Shell Structure through Galvanic Replacement Reactions. *Chem – A Eur J*. 2012;18(47):14974-14980. doi:https://doi.org/10.1002/chem.201202477

115. Watson KJ, Zhu J, Nguyen ST, Mirkin CA. Hybrid Nanoparticles with Block Copolymer Shell Structures. *J Am Chem Soc*. 1999;121(2):462-463. doi:10.1021/ja983173l

116. Cao, Jin R, Mirkin CA. DNA-Modified Core−Shell Ag/Au Nanoparticles. *J Am Chem Soc*. 2001;123(32):7961-7962. doi:10.1021/ja011342n

117. Métraux GS, Cao YC, Jin R, Mirkin CA. Triangular Nanoframes Made of Gold and Silver. *Nano Lett*. 2003;3(4):519-522. doi:10.1021/nl034097+

118. Zhang W, Callmann CE, Mirkin CA. Controlling the Biological Fate of Liposomal Spherical Nucleic Acids Using Tunable Polyethylene Glycol Shells. *ACS Appl Mater Interfaces*. 2021;13(39):46325-46333. doi:10.1021/acsami.1c12852

119. Chen J-F, Ding H-M, Wang J-X, Shao L. Preparation and characterization of porous hollow silica nanoparticles for drug delivery application. *Biomaterials*. 2004;25(4):723-727. doi:https://doi.org/10.1016/S0142-9612(03)00566-0

120. Skrabalak SE, Chen J, Au L, Lu X, Li X, Xia Y. Gold Nanocages for Biomedical Applications. *Adv Mater*. 2007;19(20):3177-3184. doi:https://doi.org/10.1002/adma.200701972

121. Chen J, Wang D, Xi J, et al. Immuno Gold Nanocages with Tailored Optical Properties for Targeted Photothermal Destruction of Cancer Cells. *Nano Lett*. 2007;7(5):1318-1322. doi:10.1021/nl070345g

122. Sokolova V V, Radtke I, Heumann R, Epple M. Effective transfection of cells with multi-shell calcium phosphate-DNA nanoparticles. *Biomaterials*. 2006;27(16):3147-3153. doi:https://doi.org/10.1016/j.biomaterials.2005.12.030

123. Cai Y, Pan H, Xu X, Hu Q, Li L, Tang R. Ultrasonic Controlled Morphology Transformation of Hollow Calcium Phosphate Nanospheres: A Smart and Biocompatible Drug Release System. *Chem Mater*. 2007;19(13):3081-3083. doi:10.1021/cm070298t

124. Shi J, Xiao Z, Votruba AR, Vilos C, Farokhzad OC. Differentially Charged Hollow Core/Shell Lipid-Polymer-Lipid Hybrid Nanoparticles for Small Interfering RNA Delivery. *Angew Chemie Int Ed*. 2011;50(31):7027-7031. doi:10.1002/anie.201101554

125. Dilebo J. Mesoporous Silica Nanoparticles Based Antigens and Nucleic Acids Delivery: A Review. *Asian J Pharm Res Dev*. 1970;8(2):50-57. doi:10.22270/ajprd.v8i2.686

126. Caruso F, Caruso RA, Mohwald H. Nanoengineering of inorganic and hybrid hollow spheres by colloidal templating. *Science*. 1998;282(5391):1111-1114. doi:10.1126/science.282.5391.1111

127. Marinakos SM, Novak JP, Brousseau LC, et al. Gold Particles as Templates for the Synthesis of Hollow Polymer Capsules. Control of Capsule Dimensions and Guest Encapsulation. *J Am Chem Soc*. 1999;121(37):8518-8522. doi:10.1021/ja990945k

128. Kim M, Sohn K, Na H Bin, Hyeon T. Synthesis of Nanorattles Composed of Gold Nanoparticles Encapsulated in Mesoporous Carbon and Polymer Shells. *Nano Lett*. 2002;2(12):1383-1387. doi:10.1021/nl025820j

129. Boyer C, Whittaker MR, Nouvel C, Davis TP. Synthesis of Hollow Polymer Nanocapsules Exploiting Gold Nanoparticles as Sacrificial Templates. *Macromolecules*. 2010;43(4):1792-1799. doi:10.1021/ma902663n

130. Yang Y, Chu Y, Yang F, Zhang Y. Uniform hollow conductive polymer microspheres synthesized with the sulfonated polystyrene template. *Mater Chem Phys*. 2005;92(1):164-171. doi:10.1016/j.matchemphys.2005.01.007

131. Kim KK, Pack DW. Microspheres for Drug Delivery. *BioMEMS Biomed Nanotechnol Vol I Biol Biomed Nanotechnol*. Published online 2006:19-50. doi:10.1007/978-0-387-25842-3_2

132. Liang H-P, Zhang H-M, Hu J-S, Guo Y-G, Wan L-J, Bai C-L. Pt hollow nanospheres: facile synthesis and enhanced electrocatalysts. *Angew Chem Int Ed Engl*. 2004;43(12):1540-1543. doi:10.1002/anie.200352956

133. Young KL, Scott AW, Hao L, Mirkin SE, Liu G, Mirkin CA. Hollow Spherical Nucleic Acids for Intracellular Gene Regulation Based upon Biocompatible Silica Shells. *Nano Lett*. 2012;12(7):3867-3871. doi:10.1021/nl3020846

134. Li Y, Li N, Pan W, Yu Z, Yang L, Tang B. Hollow Mesoporous Silica Nanoparticles with Tunable Structures for Controlled Drug Delivery. *ACS Appl Mater Interfaces*. 2017;9(3):2123-2129. doi:10.1021/acsami.6b13876

135. Ying JY, Papaefthymiou GC, Yi DK, Lee SS. Nanoparticle Architectures Templated by SiO2/Fe2O3 Nanocomposites. Published online February 7, 2006. doi:10.1021/cm0512979.s001

136. Qian H, Lin G, Zhang Y, Gunawan P, Xu R. A new approach to synthesize uniform metal oxide hollow nanospheres via controlled precipitation. *Nanotechnology*. 2007;18:355602. doi:10.1088/0957-4484/18/35/355602

137. Landon PB, Mo AH, Zhang C, et al. Designing hollow nano gold golf balls. *ACS Appl Mater Interfaces*. 2014;6(13):9937-9941. doi:10.1021/am502519x

138. Liu Q, Zhou Y, Li M, et al. Polyethylenimine Hybrid Thin-Shell Hollow Mesoporous Silica Nanoparticles as Vaccine Self-Adjuvants for Cancer Immunotherapy. *ACS Appl Mater Interfaces*. 2019;11(51):47798-47809. doi:10.1021/acsami.9b19446

139. Chang B, Sha X, Guo J, Jiao Y, Wang C, Yang W. Thermo and pH dual responsive, polymer shell coated, magnetic mesoporous silica nanoparticles for controlled drug release. *J Mater Chem*. 2011;21(25):9239-9247. doi:10.1039/C1JM10631G

140. Li Z-Z, Wen L-X, Shao L, Chen J-F. Fabrication of porous hollow silica nanoparticles and their applications in drug release control. *J Control Release*. 2004;98(2):245-254. doi:https://doi.org/10.1016/j.jconrel.2004.04.019

141. Cao Y, Wang B, Wang Y, Lou D. Dual Drug Release from Core–Shell Nanoparticles with Distinct Release Profiles. *J Pharm Sci*. 2014;103(10):3205-3216. doi:https://doi.org/10.1002/jps.24116

142. Singh N, Karambelkar A, Gu L, et al. Bioresponsive Mesoporous Silica Nanoparticles for Triggered Drug Release. *J Am Chem Soc*. 2011;133(49):19582-19585. doi:10.1021/ja206998x

143. Cao Y, Wang B, Wang Y, Lou D. Polymer-controlled core–shell nanoparticles: a novel strategy for sequential drug release. *RSC Adv*. 2014;4(57):30430-30439. doi:10.1039/C4RA03610G

144. Conley BM, Pongkulapa T, Lee K-B. Multiphase Drug Release in Hollow Multishelled Structures. *Chem*. 2020;6(11):2875-2877. doi:https://doi.org/10.1016/j.chempr.2020.10.006

145. Song W-J, Du J-Z, Sun T-M, Zhang P-Z, Wang J. Gold Nanoparticles Capped with Polyethyleneimine for Enhanced siRNA Delivery. *Small*. 2010;6(2):239-246. doi:10.1002/smll.200901513

146. Ungaro F, De Rosa G, Miro A, Quaglia F. Spectrophotometric determination of polyethylenimine in the presence of an oligonucleotide for the characterization of controlled release formulations. *J Pharm Biomed Anal*. 2003;31(1):143-149. doi:https://doi.org/10.1016/S0731-7085(02)00571-X

147. Tang M, Szoka F. The influence of polymer structure on the interactions of cationic polymers with DNA and morphology of the resulting complexes. *Gene Ther*. 1997;4(8):823-832. doi:10.1038/sj.gt.3300454

148. Yan X, Zhang Y, Zhang H, Wang PG, Chu X, Wang X. Amphiphilic polyethylenimine (PEI) as highly efficient non-viral gene carrier. *Org Biomol Chem*. 2014;12(12):1975-1982. doi:10.1039/C3OB42279H

149. Azadi S, Ashrafi H, Azadi A. Mathematical modeling of drug release from swellable polymeric nanoparticles. *J Appl Pharm Sci*. 2017;7(4):125-133. doi:10.7324/JAPS.2017.70418

150. Bohrey S, Chourasiya V, Pandey A. Polymeric nanoparticles containing diazepam: preparation, optimization, characterization, in-vitro drug release and release kinetic study. *Nano Converg*. 2016;3(1):3. doi:10.1186/s40580-016-0061-2

151. Ahmed L, Atif R, Eldeen T, Yahya I, Omara A, Eltayeb M. Study the Using of Nanoparticles as Drug Delivery System Based on Mathematical Models for Controlled Release. 2019;8:52-56.

152. Munier S, Messai I, Delair T, Verrier B, Ataman-Önal Y. Cationic PLA nanoparticles for DNA delivery: Comparison of three surface polycations for DNA binding, protection and transfection properties. *Colloids Surfaces B Biointerfaces*. 2005;43(3):163-173. doi:https://doi.org/10.1016/j.colsurfb.2005.05.001

153. Suvarna M, Dyawanapelly S, Kansara B, Dandekar P, Jain R. Understanding the Stability of Nanoparticle–Protein Interactions: Effect of Particle Size on Adsorption, Conformation and Thermodynamic Properties of Serum Albumin Proteins. *ACS Appl Nano Mater*. 2018;1(10):5524-5535. doi:10.1021/acsanm.8b01019

154. Bali K, Bak M, Szarka K, et al. Controlling the morphology of poly(ethyleneimine)/gold nanoassemblies through the variation of pH and electrolyte additives. *J Mol Liq*. 2021;322:114559. doi:https://doi.org/10.1016/j.molliq.2020.114559

155. Encabo-Berzosa MM, Sancho-Albero M, Sebastian V, et al. Polymer functionalized gold nanoparticles as nonviral gene delivery reagents. *J Gene Med*. 2017;19(6-7):e2964. doi:https://doi.org/10.1002/jgm.2964

156. He YQ, Liu SP, Kong L, Liu ZF. A study on the sizes and concentrations of gold nanoparticles by spectra of absorption, resonance Rayleigh scattering and resonance non-linear scattering. *Spectrochim Acta Part A Mol Biomol Spectrosc*. 2005;61(13):2861-2866. doi:https://doi.org/10.1016/j.saa.2004.10.035

157. Hajian R, Shams N, PARVIN A. DNA-binding Studies of Daunorubicin in the Presence of Methylene Blue by Spectroscopy and Voltammetry Techniques. *Chinese J Chem*. 2009;27:1055-1060. doi:10.1002/cjoc.200990176

158. Grenda K, Idström A, Evenäs L, Persson M, Holmberg K, Bordes R. An analytical approach to elucidate the architecture of polyethyleneimines. *J Appl Polym Sci*. 2022;139(7):51657. doi:10.1002/app.51657

159. Whitener R, Mosley RJ, Wower J, Byrne ME. Nucleic acid biohybrid nanocarriers with high-therapeutic payload and controllable extended release of daunomycin for cancer therapy. *J Biomed Mater Res - Part A*. 2021;109(7):1256-1265. doi:10.1002/jbm.a.37119

160. Mahajan S, Tang T. Polyethylenimine–DNA Nanoparticles under Endosomal Acidification and Implication to Gene Delivery. *Langmuir*. 2022;38(27):8382-8397. doi:10.1021/acs.langmuir.2c00952

161. Butowska K, Woziwodzka A, Borowik A, Piosik J. Polymeric Nanocarriers: A Transformation in Doxorubicin Therapies. *Materials (Basel)*. 2021;14(9):2135. doi:10.3390/ma14092135

162. Zunino F, Di Marco A, Zaccara A, Gambetta RA. The interaction of daunorubicin and doxorubicin with DNA and chromatin. *Biochim Biophys Acta - Nucleic Acids Protein Synth*. 1980;607(2):206-214. doi:https://doi.org/10.1016/0005-2787(80)90073-8

163. Carlson HA, Smith RD, Khazanov NA, Kirchhoff PD, Dunbar JBJ, Benson ML. Differences between high- and low-affinity complexes of enzymes and nonenzymes. *J Med Chem*. 2008;51(20):6432-6441. doi:10.1021/jm8006504

164. Graves DE, Krugh TR. Adriamycin and daunorubicin bind in a cooperative manner to deoxyribonucleic acid. *Biochemistry*. 1983;22(16):3941-3947. doi:10.1021/bi00285a033

165. Sharma A, Cornejo C, Mihalic J, et al. Physical characterization and in vivo organ distribution of coated iron oxide nanoparticles. *Sci Rep*. 2018;8(1). doi:10.1038/s41598-018-23317-2

166. Tamkovich SN, Cherepanova A V, Kolesnikova E V, et al. Circulating DNA and DNase activity in human blood. *Ann N Y Acad Sci*. 2006;1075:191-196. doi:10.1196/annals.1368.026

167. Teva Parental Medicines Inc. DAUNORUBICIN HYDROCHLORIDE INJECTION. Published online 2012. https://dailymed.nlm.nih.gov/dailymed/drugInfo.cfm?setid=29fe455e-f177-4b0e-99fb-60a53016db72

Appendix A

Supplemental Data

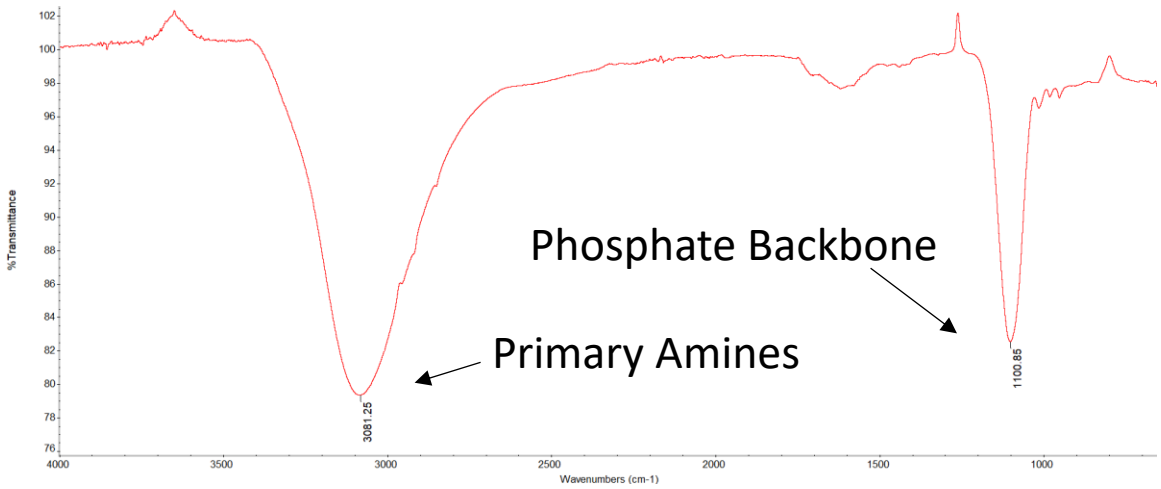

Figure A1. FTIR detection of HCPPs with DNA condensed to the surface. 75 mg of copper is used per 1 mL of HCPPs. The aggregates of 32 individual runs are aggregated, and a background measurement is collected before data collection. Data points indicate the wavelength at which the peak occurs.

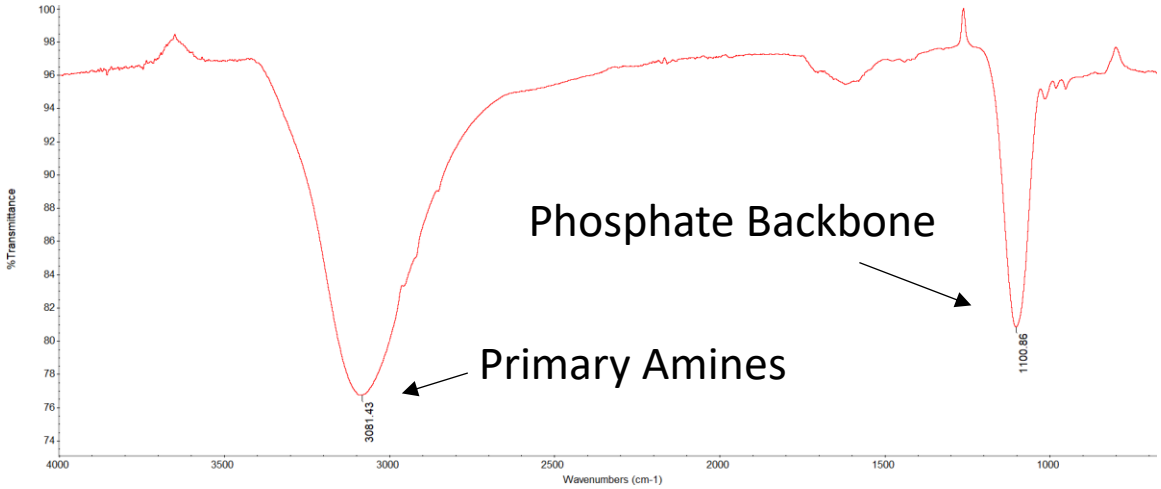

Figure A2. FTIR detection of HCPPs with daunorubicin loaded DNA condensed to the surface. 75 mg of copper is used per 1 mL of HCPPs. The aggregates of 32 individual runs are aggregated, and a background measurement is collected before data collection. Data points indicate the wavelength at which the peak occurs.

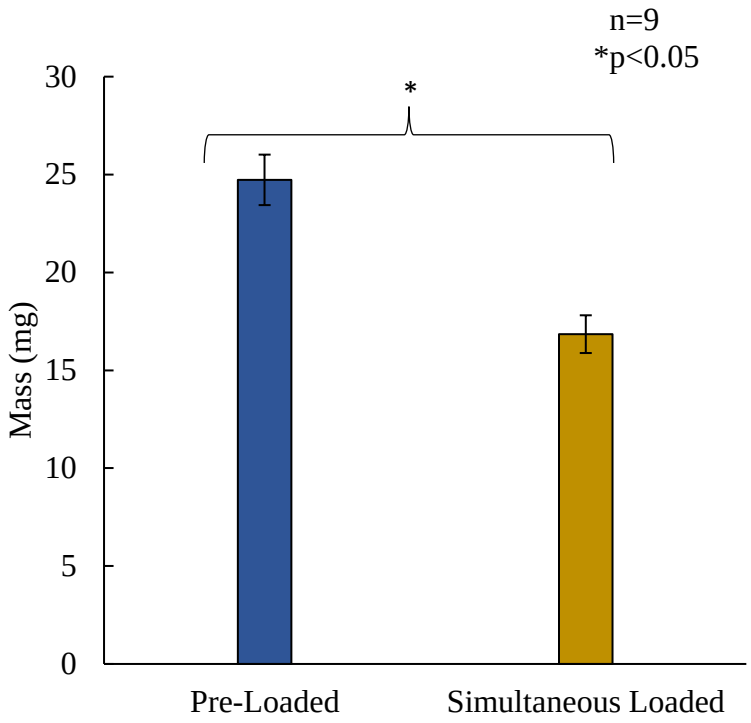

Figure A3. Mass changes in pre-loaded and simultaneously drug loaded DNA to HCPPs. One-way Anova testing is used to determine significance. Pre-Loaded DNA (■) is given one hour to allow for enough intercalation of daunorubicin to the nucleotides before mixing with HCPPs for one hour. Simultaneously loaded DNA (■) is introduced to a solution containing both DNA and the HCPPs, then given two hours of mixing time.

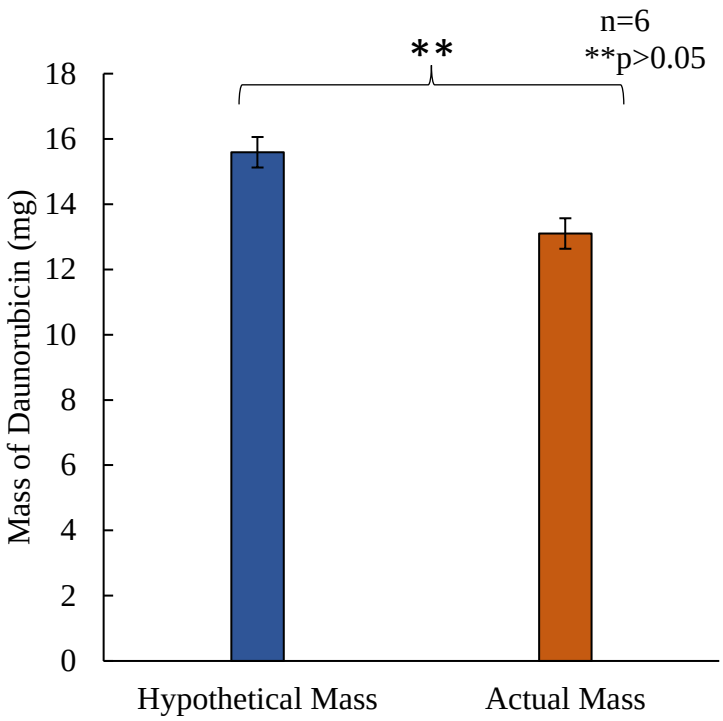

Figure A4. Hypothetical mass of daunorubicin loaded to hollow core vs. actual mass loaded. The hypothetical mass of daunorubicin able to load to the particle interior (■) was compared to the actual mass found to load to the particle interior (■). The total volume of the nanoparticle and the hollow core was calculated to determine the total volume of available space for loading. The density of daunorubicin was further used to determine the hypothetical amount of mass capable of loading to the particle interior. This was compared to the difference in mass found experimentally between the hollow core particle and the solid core formulation. Significance was determined through One-way Anova testing.